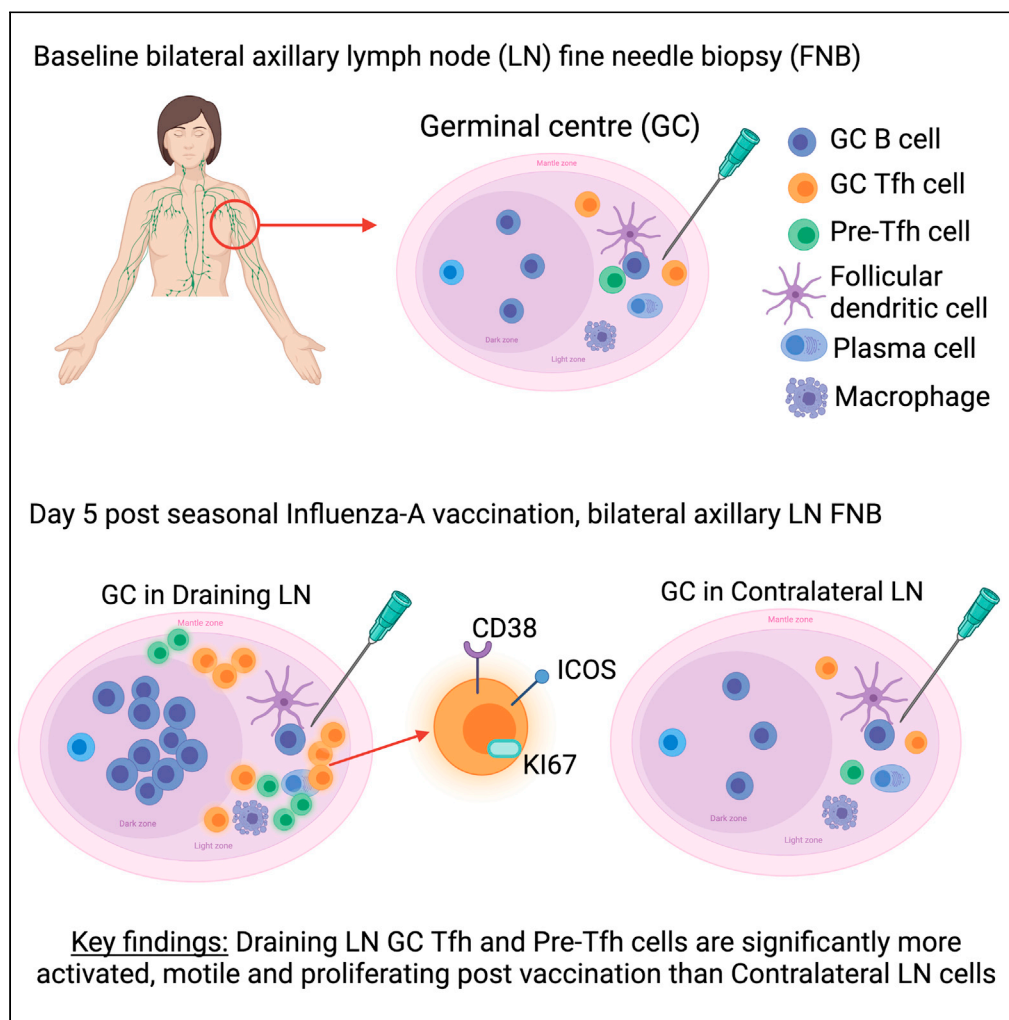


Article

Early expansion of CD38+ICOS+ GC Tfh in draining lymph nodes during influenza vaccination immune response



Hannah Law,
Melanie Mach,
Annett Howe, ...,
John Zaunders,
Anthony D.
Kelleher, C. Mee
Ling Munier

hlaw@kirby.unsw.edu.au (H.L.)
cmunier@kirby.unsw.edu.au
(C.M.L.M.)

Highlights

Early response to
influenza vaccine is
characterized by
expansion of GC cell
subsets

Specific expansion of
CD38+ ICOS+ GC Tfh and
Pre-Tfh occurs in draining
LNs only

Activated GC Tfh and Pre-
Tfh are also proliferating,
expressing high levels of
Ki67

Correlation between
activated Pre-Tfh and
activated c-Tfh suggests a
potential origin

Law et al., iScience 25, 103656
January 21, 2022 © 2021 The
Author(s).
[https://doi.org/10.1016/
j.isci.2021.103656](https://doi.org/10.1016/j.isci.2021.103656)

Article

Early expansion of CD38⁺ICOS⁺ GC Tfh in draining lymph nodes during influenza vaccination immune response

Hannah Law,^{1,*} Melanie Mach,^{1,2} Annett Howe,¹ Solange Obeid,³ Brad Milner,³ Cate Carey,¹ Maxine Elfis,³ Bertha Fsadni,⁴ Katherine Ognenovska,¹ Tri Giang Phan,^{5,6} Diane Carey,¹ Yin Xu,¹ Vanessa Venturi,¹ John Zaunders,^{1,4,7} Anthony D. Kelleher,^{1,3,4,7,8} and C. Mee Ling Munier^{1,7,8,*}

SUMMARY

T follicular helper (Tfh) cells provide critical help to B cells during the germinal center (GC) reaction to facilitate generation of protective humoral immunity. Accessing the human lymph node (LN) to study the commitment of CD4 T cells to GC Tfh cell differentiation during *in vivo* vaccine responses is difficult. We used ultrasound guided fine needle biopsy to monitor recall responses in axillary LNs to seasonal influenza vaccination in healthy volunteers. Specific expansion of GC cell subsets occurred exclusively within draining LNs five days postvaccination. Draining LN GC Tfh and precursor-Tfh cells express higher levels of CD38, ICOS, and Ki67, indicating they were significantly more activated, motile, and proliferating, compared to contralateral LN cells. These observations provide insight into the early expansion phase of the human Tfh lineage within LNs during a vaccine induced memory response and highlights early LN immune responses may not be reflected in the periphery.

INTRODUCTION

Adaptive immunity is mediated by the coordinate action of multiple components, for the generation of memory B cells, antibodies (Abs), memory CD8⁺, and CD4⁺ T lymphocytes (Krammer et al., 2018). The production of neutralizing Abs by plasma cells is dependent on B cells undergoing affinity maturation as part of the germinal center (GC) reaction within secondary lymphoid tissues (Inoue et al., 2018; Shinnakasu and Kurosaki, 2017). Within GCs, T follicular helper (Tfh) cells are defined as CXCR5^{high} PD-1^{high} Bcl6^{high} memory CD4⁺ T cells (Yu et al., 2009; Perreau et al., 2013; Fazilleau et al., 2009). Tfh cells provide critical help to GC B cells during somatic hypermutation and affinity maturation to produce high affinity, class-switched antibodies and to develop immunological memory (Crotty, 2014; Vinuesa et al., 2005; Fazilleau et al., 2007). However, the inaccessible anatomical location of Tfh cells, within the GC of lymphoid tissue, poses a considerable barrier to studying their role in human immune responses in real time. This location is particularly challenging to the longitudinal study of Tfh cells in the context of vaccination, a goal that is even more pertinent following the outbreak of SARS-CoV-2.

Numerous studies of mouse lymphoid tissue via serial sacrifice and harvesting of lymphoid tissues have yielded substantial and important information (Harker et al., 2011; Poovassery and Moore, 2006). Various animal models have allowed careful inspection of the architecture of lymph nodes (Rezende et al., 2019; Schudel et al., 2019), illuminating the importance of cell positioning and the micro-circulation within lymph nodes in the generation of effective immune responses (Miller et al., 2002; Lopez et al., 2020; Pizzagalli et al., 2019; Suan et al., 2015; Moran et al., 2018). One informative murine study demonstrated that Tfh cell recall responses peak at day 5 postvaccination, 2 days before the peak of the GC B cell population (Suan et al., 2015). Another study reported expansion of hemagglutinin (HA)-specific GC B cells as early as four days postvaccination, but saw no expansion of the Tfh cell population (Kil et al., 2019). However, such studies are challenging in humans as serial harvesting of whole lymph nodes has high potential for morbidity. In an effort to overcome this limitation, many studies have sought to utilize more easily accessible alternatives, such as postoperative tonsils or spleens for cross sectional studies, whereas longitudinal studies have often used a phenotypically similar surrogate cell known as circulating-Tfh (c-Tfh) that can be detected in peripheral blood (Ma and Phan, 2017).

¹The Kirby Institute, UNSW Sydney, Sydney 2052, NSW, Australia

²The University of Sydney, Sydney 2006, NSW, Australia

³St Vincent's Hospital Sydney, Sydney 2010, NSW, Australia

⁴St Vincent's Centre for Applied Medical Research (AMR), Sydney 2010, NSW, Australia

⁵Garvan Institute of Medical Research, Sydney 2010, NSW, Australia

⁶St Vincent's Clinical School, Faculty of Medicine, UNSW Sydney, Sydney 2010, NSW, Australia

⁷These author contributed equally

⁸Lead contact

*Correspondence: hlaw@kirby.unsw.edu.au (H.L.), cmunier@kirby.unsw.edu.au (C.M.L.M.)

<https://doi.org/10.1016/j.isci.2021.103656>



The identification of c-Tfh, within the peripheral blood, has proven to be useful as an easily accessible biomarker for immune responses (Bentebibel et al., 2013; Locci et al., 2013). Multiple studies have since demonstrated the emergence of a transient population of PD-1+ICOS + c-Tfh cells following vaccination with inactivated influenza virus (Bentebibel et al., 2013; Herati et al., 2014, 2017; Koutsakos et al., 2018). Levels of c-Tfh cells peak at day 7 and correlate with Ab serum titers as well as antigen-specific B cell and antibody secreting cell (ASCs) numbers (Koutsakos et al., 2018; Herati et al., 2014, 2017). c-Tfh cells have also been shown to correlate with increased antibody avidity, suggesting these cells may be involved in the generation of more effective immune responses (Bentebibel et al., 2016). Inactivated influenza virus-induced c-Tfh cells were phenotypically similar to their GC counterparts, expressing various activation markers including PD-1, CD38, ICOS, and Ki67 (Pilkinton et al., 2017; Herati et al., 2014, 2017). The most convincing studies thus far have demonstrated a relationship between c-Tfh and GC Tfh through immunophenotyping, T cell receptor repertoire analysis, and single cell transcriptomics (Brenna et al., 2020; Hill et al., 2019). Taken together, these results suggest that c-Tfh are a potential surrogate for GC Tfh and immune responses in the LN. However, lack of longitudinal studies assessing correlation of parallel tissues and peripheral blood means a definitive relationship between these cell groups is yet to be established.

Our group has pioneered the utilization of fine needle biopsies (FNBs) in macaques and human inguinal LNs to investigate Tfh and GC B cells during SIV and HIV infection, respectively (Hey-Nguyen et al., 2017; Xu et al., 2013a; Zaunders et al., 2017). These studies allowed detailed analysis of GC expansion in these infections, compared to lymph nodes in uninfected individuals, and complemented other studies of progressive infection of Tfh in the context of SIV and HIV infection (Xu et al., 2017; Zaunders et al., 2017), which suggested that infection of Tfh could occur at an early activated stage of Pre-Tfh cell development.

Subsequent studies have also adopted the FNB technique to study immune responses to vaccination in macaques (Havenar-Daughton et al., 2016) and GC B cell responses to vaccination in humans to influenza (Turner et al., 2020) and SARS-CoV-2 (Turner et al., 2021). This study used FNB sampling, at baseline and day 5 postvaccination, to understand the earliest changes in the T cell compartment, focusing on the commitment of memory CD4 T cells to the GC Tfh cell lineage in response to seasonal tetra-valent influenza vaccination in axillary LNs of healthy individuals with previous exposure to influenza antigens. Further, we investigated differences between draining and contralateral LNs, with an aim to more clearly define the nature of the draining LN response. Finally, this study aimed to determine if the identification of influenza specific CD4+ T cells in peripheral blood was reflective of GC responses five days postvaccination within the draining LN, to better understand the bifurcation between immediate GC Tfh cells and generation of effector/memory antigen-specific CD4 T cells for peripheral surveillance.

RESULTS

Longitudinal LN FNB are reliable and well-tolerated

LN FNB was successfully performed on 26 healthy individuals, with evidence of previous exposure to the HA protein of influenza (mean [SD] HAI titer: 44 [32]), without any serious adverse events. Some participants reported mild, transient local discomfort lasting hours or mild bruising lasting 2–3 days. A total of 93 biopsies were performed. Participant information is summarized in Table S1. The median age of participants was 35 years and 52% of participants were male. Axillary LN sizes sampled in this study ranged from 2.6mm to 11.6mm (median: 5.2mm) in length.

Seven biopsies collected from 3 participants were used for assay optimization and were therefore excluded from further data analysis. One participant did not continue with the study past baseline because of COVID-19 induced shut down of non-essential radiological services.

Among the remaining 22 healthy volunteers, 84 biopsies were attempted and 71 were successful, as assessed by total lymphocyte count and absence of blood contamination. Of the 13 biopsies deemed unsuccessful, one was because of the inability to locate a suitable node via ultrasound for sampling and 12 were attempted but no cells were recovered. As a result of unsuccessful draining and contralateral baseline LN biopsies in two participants, a total of 4 postvaccination biopsies were not attempted.

Quality control of LN FNB

LN FNB viability after culture with no antigen at 44 h post collection is shown in [Figure S1](#). This is representative of 16 LN FNB samples where the median viability of cells was 99.25% (range = 95.6%–100%). Blood contamination of FNB samples may skew results and is associated with the use of aspiration and increased frequency of sampling ([Murali et al., 2010](#)). Quality control of LN FNBs is of particular importance for interrogation of cell subsets of bone fide LN Tfh cells, as distinct from c-Tfh, and rare cells in LNs, including pDCs and T regulatory cells. To assess if substantial blood contamination existed in our longitudinal FNB samples, the frequency of CD3-CD56+ CD16 + natural killer (NK) cells, CD45 + neutrophils and CD3+CD14 + monocytes from peripheral blood (PB) ([Figure S2A](#)) was compared to FNB samples ([Figure S2B](#)), revealing very low levels of these cell types in the LN FNB samples ([Figure S2B](#)). NK cell, neutrophil, and monocyte to lymphocyte ratios in LN and PB samples are shown in [Figures S2C–S2E](#).

Lymphocyte cell number was used as the primary indicator of the success and yield from LN FNB samples. Total lymphocyte cell number ranged from 6.8×10^3 to 12.2×10^6 in the LN FNB samples (median = 1.1×10^6) and 4.9×10^6 to 20.3×10^6 from the 6mLs of the peripheral blood collected (median = 11.2×10^6 ; [Figure S2F](#)). T lymphocyte subset frequencies and medians for LN and PB samples are discussed in supplementary data and presented in [Figure S2G](#). Overall, these results are consistent with LN composition reported in the literature and confirm that there is little blood contamination within the longitudinal LN FNB samples ([Xu et al., 2013a](#); [Hey-Nguyen et al., 2017](#)).

Expansion of absolute Tfh cell numbers postvaccination in draining LNs

The FNB technique provides reliable detection of a distinct population of Tfh cells without excision of the lymph node, therefore enabling investigation of vaccine-induced immune responses. Germinal Center (GC) Tfh cells were identified as CD3+CD4+CD45RA-CD25^{low}CD127-PD-1^{high}CXCR5^{high} ([Figure 1A](#); red box). Precursor Tfh cells (Pre-Tfh), were identified as CD3+CD4+CD45RA-CD25^{low}CD127-PD-1^{medium}-CXCR5^{medium} ([Figure 1A](#); purple box).

At baseline, the absolute number of Tfh cells in LN FNB samples ranged from 30 to 30,536 cells, with a median cell number of 2,443. Five days post influenza vaccination (day 5), absolute number of Tfh cells in LN FNBs ranged from 333 to 85,127 cells, with a median cell number of 4,864. There was no difference in Tfh cells as a proportion of CD4+ T cells between timepoints, presumably because of the expansion of the whole LN following vaccination. However, the absolute number of Tfh cells in the draining lymph node was significantly higher at day 5 postvaccination when compared to baseline ([Figure 2A](#)). There was no significant difference in Tfh cell number between timepoints in the contralateral LN. Further, at day 5 the number of Tfh cells was significantly higher in draining LNs than in contralateral LNs ([Figure 2B](#)).

The Pre-Tfh cell population was of particular interest in this study because of their role in the development of Tfh and their potential contribution to the memory CD4+ T cell population ([Trub et al., 2017](#)). At baseline, the absolute number of Pre-Tfh cells in LN FNB samples ranged from 252 to 616,420 cells, with a median cell number of 13,152. Five days post influenza vaccination, absolute number of Pre-Tfh cells in LN FNBs ranged from 2,131 to 241,053 cells, with a median cell number of 20,784. Interestingly, we saw no difference in absolute number of Pre-Tfh cells between baseline and day 5 in either draining or contralateral LNs ([Figure 2C](#)). Further, there was no difference in absolute number of Pre-Tfh cells between draining and contralateral LNs at day 5 postvaccination ([Figure 2D](#)).

Expression of the Tfh lineage transcription factor, Bcl6, was measured to identify the presence of a transcriptional relationship between Pre-Tfh and GC Tfh cells (reviewed in [[Suh, 2015](#)]). The proportion of GC Tfh cells expressing Bcl6 in draining LNs was significantly higher than the proportion of their circulating counterparts c-Tfh in PB expressing this transcription factor ([Figure 2E](#)). Interestingly, there was no significant difference between the frequency of Bcl6+ Pre-Tfh and Bcl6+ Tfh cells at baseline or day 5 ([Figure 2E](#)), which suggests Pre-Tfh cells were following the Tfh differentiation pathway.

Because of the interdependent relationship of GC Tfh and GC B cells, we investigated expansion of the GC B cell population. Here, GC B cells were identified as CD3-CD20+ CD38^{high}Bcl6+ ([Figure 1B](#); red box). At baseline, absolute number of GC B cells ranged from 64 to 43,300 cells, with a median cell number of 5,286. Postvaccination (day 5), the absolute number of GC B cells ranged from 117 to 232,615 cells, with a median cell number of 6,957. The difference in absolute GC B cells between baseline and day 5 was not significant

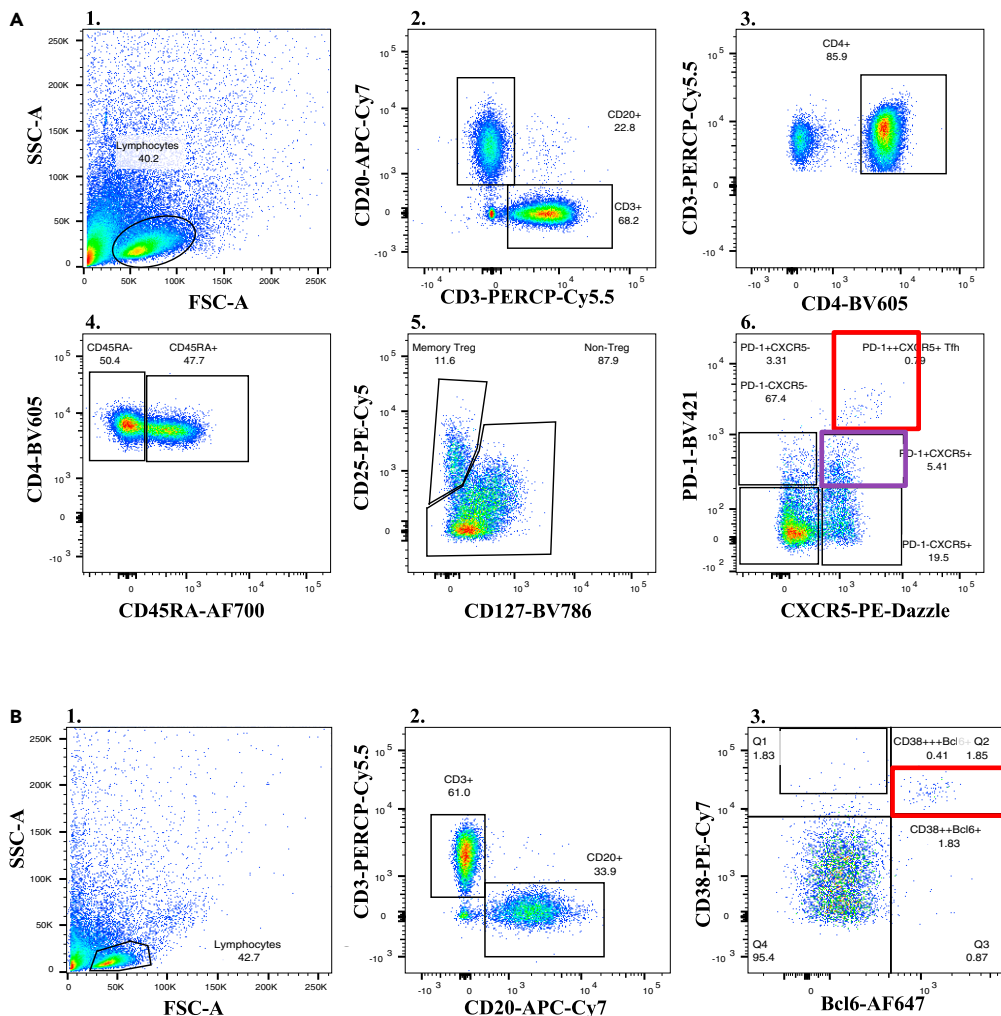


Figure 1. GCTfh cell, Pre-Tfh cell, and GC B cell gating strategy

(A) Lymphocytes were identified using SSC versus FSC. The gated lymphocyte population was then plotted on CD20 versus CD3 to identify CD3+CD20- T cells. CD3+ T cells were then further plotted for CD4 expression to identify CD3+CD4+ T cells. CD45RA was then used to identify the CD3+CD4+CD45RA-memory T cells. Memory CD4+ T cells were plotted for CD25 and CD127 expression to exclude the CD25^{high} CD127- T regulatory cells from further analysis. Finally, CD25^{low}CD4+CD45RA- T cells were then plotted for PD-1 versus CXCR5 to identify the PD-1^{high}CXCR5+ GC Tfh cells (red box). From this plot, precursor Tfh cells (Pre-Tfh) were also identified as PD-1^{medium} CXCR5^{medium} cells (purple box).

(B) Lymphocytes were identified using SSC versus FSC. The gated lymphocyte population was then plotted on CD20 versus CD3 to identify CD20+ CD3- B cells. CD20+ B cells were then plotted on CD38 versus Bcl6 expression to identify the CD38^{high}Bcl6+CD20+ B cells (red box). See also [Figures S1](#) and [S2](#).

in draining or contralateral LNs ([Figure 2F](#)). However, interestingly, the absolute number of GC B cells was significantly higher in draining LNs compared to contralateral LNs at day 5 ([Figure 2G](#)). Collectively, these results suggest that a booster vaccination induces specific expansion of GC Tfh in the draining LN and highlights the presence of a larger GC B cell population in draining LNs post vaccination.

Postvaccination activation of GC Tfh and Pre-Tfh cells in draining LNs

We next studied activation of GC Tfh and Pre-Tfh in draining LNs, using the activation markers CD38 and ICOS, which have been linked to Tfh cell differentiation and the GC reaction (reviewed in [Wikenheiser and Stumhofer, 2016](#)). Initial analysis of the proportion of cells expressing CD38 revealed no significant difference between baseline and day 5 postvaccination in CD38+ GC Tfh as a proportion of CD4+ T cells and a significant decrease in

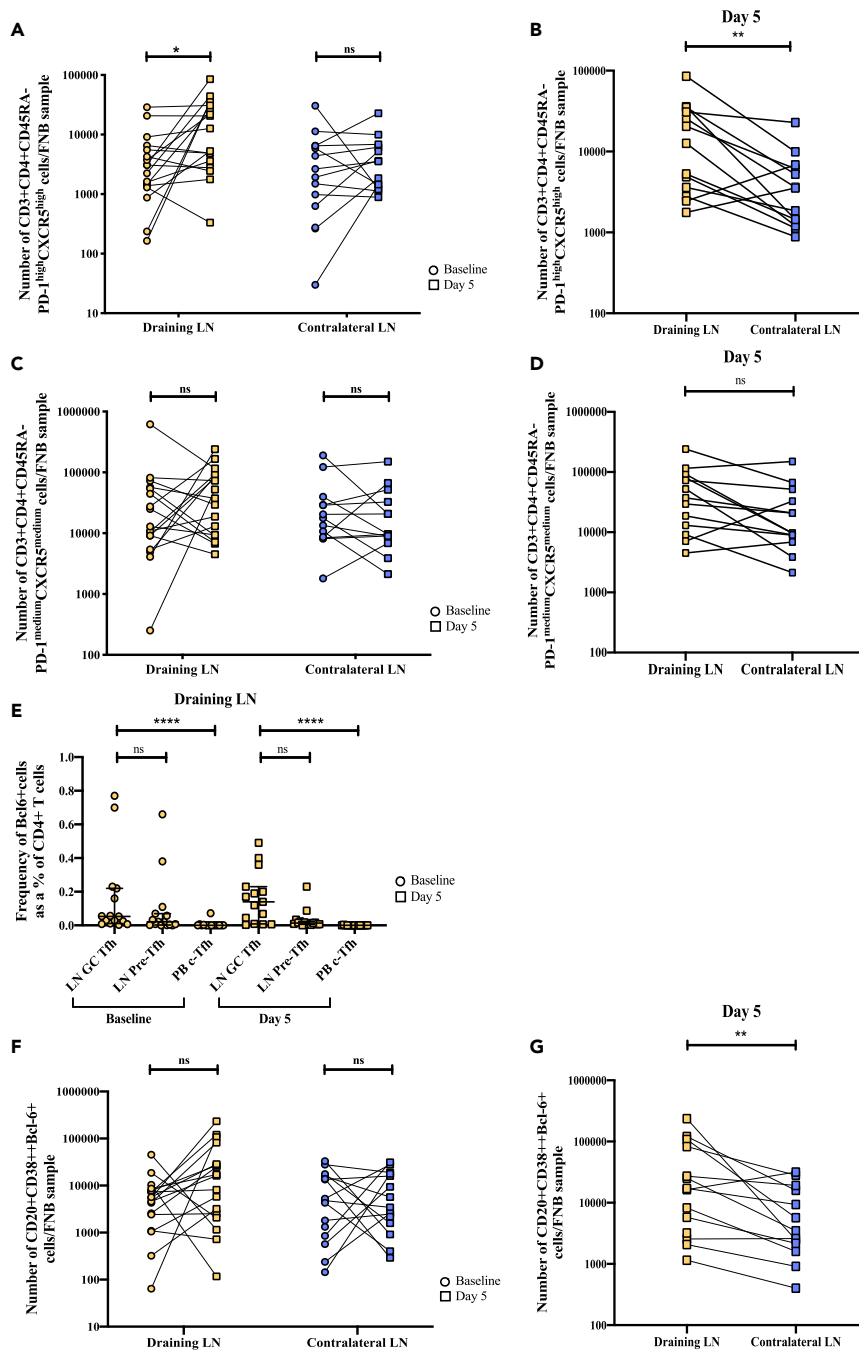


Figure 2. Absolute number of lymph node resident subsets

(A) Absolute numbers of GC Tfh cells were significantly higher at day 5 when compared to baseline in draining LNs. There was no difference in GC Tfh cell number in contralateral LNs.

(B) GC Tfh cell numbers at day 5 postvaccination were significantly higher in draining LNs than in contralateral LNs.

(C) There was no significant difference in absolute number of Pre-Tfh cells between baseline and day 5 in either draining or contralateral LNs.

(D) No significant difference between Pre-Tfh cell numbers in draining LNs compared to contralateral LNs postvaccination.

(E) Frequency of Bcl6+ Tfh were significantly higher than frequency of Bcl6+ c-Tfh from PB. There was no significant difference between frequency of Bcl6+ Tfh and Bcl6+ Pre-Tfh subsets.

(F) No difference in absolute number of GC B cells between baseline and day 5 in either draining or contralateral LNs.

Figure 2. Continued

(G) Absolute number of GC B cells were significantly higher in draining LNs compared to contralateral LNs at day 5. *, $p < 0.05$; **, $p < 0.01$; ***, $p < 0.001$; ****, $p < 0.0001$ (Wilcoxon signed rank [A-C, E, F] and Friedman's test followed by Dunn's multiple comparisons post-tests [D], median and IQR [E]).

CD38+ Pre-Tfh cells as a proportion of CD4+ T cells in both draining and contralateral LNs postvaccination (Figure S3A). Further, there was no significant difference between baseline and postvaccination in proportion of ICOS+ GC Tfh or ICOS+ Pre-Tfh in draining or contralateral LNs (Figure S3B).

However, the CD38 expression on GC Tfh, measured by Median Fluorescence Intensity (MFI) was significantly higher in draining LNs compared to contralateral LNs at day 5 postvaccination, with no difference seen at baseline (Figure 3A). The median difference in Tfh CD38 MFI between draining and contralateral LN was 481.5 at baseline and was 3797.5 at day 5. There was a statistically significant greater difference in CD38 MFI between draining and contralateral nodes at day 5 than at baseline (median of differences = 3260, $p = 0.0005$).

Within the Pre-Tfh population, CD38 MFI was also significantly higher in draining LNs compared to contralateral LNs at day 5 (Figure 3B). In addition, the difference in CD38 MFI between draining and contralateral LN was greater at day 5 than at baseline (median difference at baseline = 39; median difference at day 5 = 331; median of differences = 256.5) but these differences were not statistically significant ($p = 0.077$).

There was no difference in ICOS MFI before vaccination, between draining and contralateral LNs for both Tfh (Figure 3C) and Pre-Tfh cells (Figure 3D). However, at day 5 postvaccination, ICOS MFI was significantly higher in draining LNs compared to contralateral LNs on both Tfh cells (Figure 3C) and Pre-Tfh cells (Figure 3D).

The differences in ICOS MFI between draining and contralateral nodes were statistically significantly higher postvaccination compared to baseline in Tfh cells (median difference at baseline = 13.5; median difference at day 5 = 1487; median of differences = 1329, $p = 0.0085$). The difference in LN ICOS MFI on Pre-Tfh cells was also significantly higher at day 5 (median difference at baseline = -24.7; median difference at day 5 = 897; median of differences = 657, $p = 0.0031$).

The process of identification of CD38+ ICOS+ GC Tfh cells is represented in Figure 3E. At day 5 in the draining LN, the frequencies of both CD38+ ICOS+ GC Tfh and Pre-Tfh cells were significantly higher than baseline (Figure 3F). Importantly, in contrast, there was no difference in the frequency of either population in contralateral LNs between baseline and day 5 (Figure 3F). Furthermore, the frequency of activated and proliferating Tfh and Pre-Tfh cells measured by CD38 + Ki67+ co-expression, was significantly higher at day 5 compared to baseline in draining LNs exclusively (Figure 3G).

Overall, the qualitative changes of Tfh populations postvaccination in the draining LN only, support our hypothesis that frequency of Tfh cells, and frequency of the CD38+ ICOS+ GC Tfh population by extension, is not detected because of the overall expansion of the cellularity of the LN in response to antigen stimulation. These results further demonstrate that the very early immune response to vaccination is restricted to the draining LN.

GC B cells, GC Tfh cells, and CD38 + ICOS + Tfh cells in draining LNs postvaccination

The interdependent relationship between GC Tfh and GC B cells is a crucial factor in the generation of effective immune responses. We found a strong, significant correlation between GC Tfh cell and GC B cell number in draining LNs (Figure 4A), but not in the contralateral LNs at day 5 postvaccination (Figure 4B). Similarly, we observed a significant positive correlation between the number of CD38+ ICOS+ Tfh cells/FNB and the number of GC B cells/FNB from draining (Figure 4C), but not contralateral LNs at day 5 postvaccination (Figure 4D). These results further support the early immune response to vaccination occurring exclusively in the draining LNs.

Successful detection of lymph node resident subsets

T follicular regulatory (Tfr) cells have been implicated in regulating the LN response to vaccination (reviewed in [Huang et al., 2020]). Tfr cells can be divided into three distinct groups based on their expression

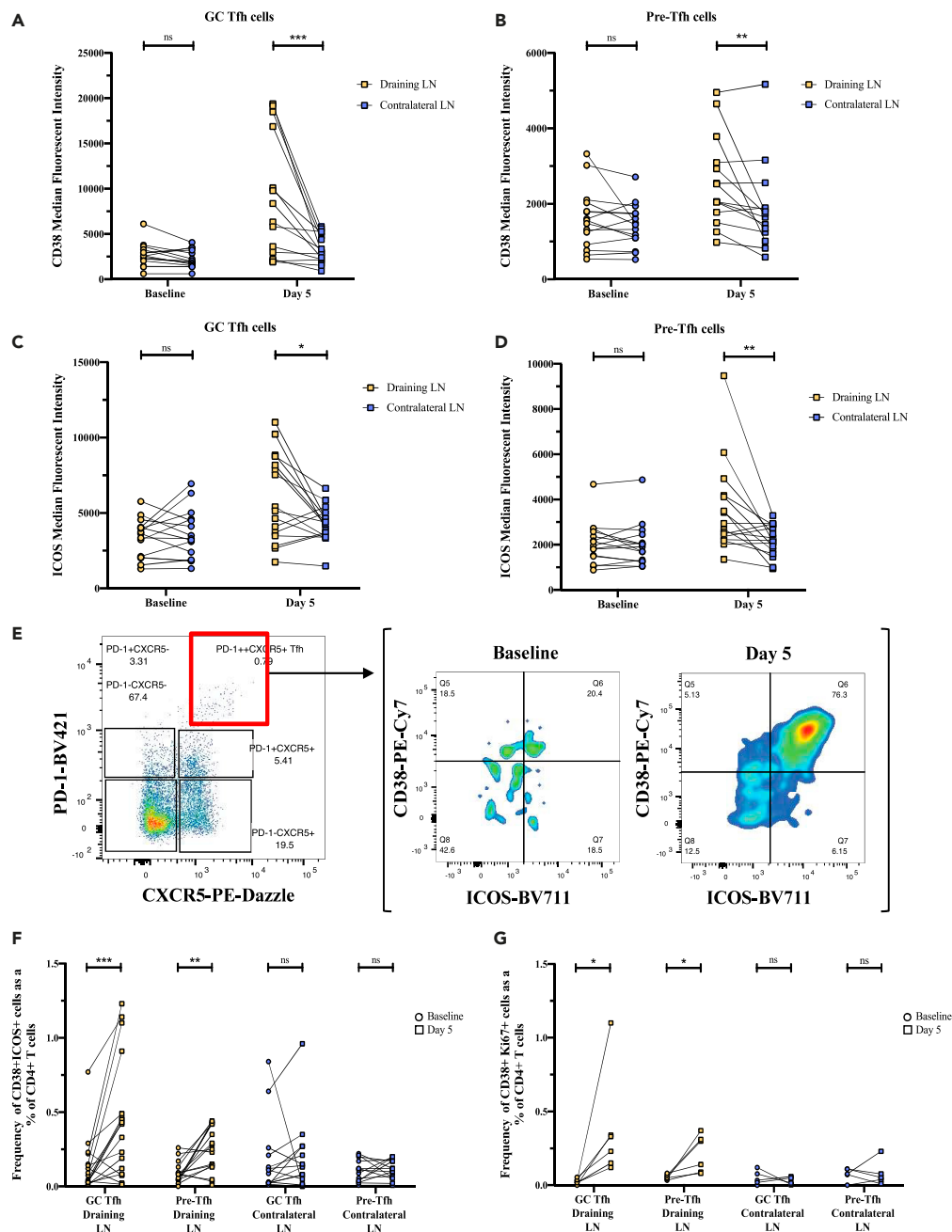


Figure 3. Activation of GC Tfh and Pre-Tfh cells in Draining LNs

(A) No significant difference in MFI of CD38 between draining and contralateral LNs in GC Tfh cells at baseline. Postvaccination, CD38MFI was significantly higher in draining LN GC Tfh cells than in contralateral LN GC Tfh cells.

(B) At baseline, no significant difference in MFI of ICOS was observed between draining and contralateral LNs in Pre-Tfh cells. Postvaccination, CD38 MFI was significantly higher in Pre-Tfh cells from draining LNs compared to contralateral LNs.

(C) No significant difference in MFI of ICOS between draining and contralateral LNs in GC Tfh cells at baseline. At day 5 postvaccination, there was a significant difference in CD38 MFI between draining and contralateral LNs on GC Tfh cells.

(D) No significant difference in MFI of ICOS between draining and contralateral LNs in Pre-Tfh cells. At day 5 postvaccination, there was a significant difference in ICOS MFI between draining and contralateral LNs on Pre-Tfh cells.

(E) Representative flow cytometry plot of CD38+ ICOS+ gating from GC Tfh cell identification.

(F) Frequency of CD38+ ICOS+ GC Tfh and CD38+ ICOS+ Pre-Tfh were significantly higher at day 5 postvaccination compared to baseline in draining LNs. No significant difference was observed between baseline and day 5 frequencies of CD38+ ICOS+ GC Tfh and CD38+ ICOS+ Pre-Tfh in contralateral LNs.

Figure 3. Continued

(G) Frequency of CD38+ Ki67+ GC Tfh and CD38+ Ki67+ Pre-Tfh cells were significantly higher at day 5 compared to baseline in draining LNs. No significant difference between baseline and day 5 CD38+ Ki67+ GC Tfh frequencies and CD38+ Ki67+ Pre-Tfh frequencies was observed in contralateral LNs. *, $p < 0.05$; **, $p < 0.01$; ***, $p < 0.001$; ****, $p < 0.0001$ (Wilcoxon signed rank). See also [Figure S3](#).

of surface proteins PD-1, CXCR5, ICOS, and transcription factor Bcl6. LN FNB can successfully identify GC Tfr (CD3+CD4+CD45RA-CD25^{high}CD127-PD-1^{high}CXCR5+Bcl6+ICOS+), Follicular Tfr (CD3+CD4+CD45RA-CD25^{high}CD127-PD-1^{medium} CXCR5+Bcl6+ICOS+), and T cell zone Tfr (CD3+CD4+CD45RA-CD25^{high}CD127-PD-1^{low}CXCR5+Bcl6-ICOS-). Identification of these Tfr subsets is shown in [Figure S4](#). Previous studies have typically utilized a circulating counterpart, termed c-Tfr, which has been reported to increase in healthy individuals following influenza vaccination ([Fonseca et al., 2017](#); [Dhaeze et al., 2015](#)).

Identification and quantification of plasmacytoid dendritic cells (pDCs) in LN FNBs was achieved consistently ([Figure 5A](#)). This is consistent with the previous description of upregulation of CCR7 expression by activated pDC ([Seth et al., 2011](#)), their migration to the LN and their role in T cell activation during the immune response ([Cella et al., 2000](#)). There was no significant difference in absolute number of pDCs between baseline and day 5 in draining or contralateral LNs ([Figure 5B](#)). Draining LNs had significantly higher absolute numbers of pDCs at day 5 compared to the contralateral LNs ([Figure 5C](#)). Further a positive correlation between absolute number of pDCs and absolute number of GC Tfh cells was observed in draining ([Figure 5D](#)), but not contralateral LNs postvaccination ([Figure 5E](#)). These results demonstrate the FNB technique is able to detect rare subsets implicated in effective immune responses, which are restricted to draining LNs.

Identification of circulating-Tfh cells (c-Tfh) in peripheral blood

In addition to investigating LN resident populations, we analyzed the c-Tfh cell population in PB with the aim of assessing the use of c-Tfh as a surrogate for GC Tfh. In this study, the phenotypic definition of c-Tfh cells in peripheral blood was the same for LN-derived Tfh cells, using the following surface proteins; CD3+CD4+CD45RA-CD25^{low}CD127-PD-1^{high}CXCR5+ T cells. There was no significant difference in frequency of c-Tfh cells between the two timepoints we considered ([Figure S5A](#)). At baseline, positive correlations between frequency of c-Tfh cells and frequency of GC Tfh cells from both the draining LN ([Figure 6A](#)) and the contralateral LN ([Figure S5B](#)) were observed. Although a significant positive correlation between c-Tfh and contralateral LN GC Tfh was upheld at day 5 postvaccination ([Figure S5C](#)), there was no significant correlation between c-Tfh and GC Tfh cells in draining LNs ([Figure 6B](#)). A significant positive correlation between c-Tfh and Pre-Tfh cells from draining LNs was observed at baseline and day 5 postvaccination ([Figures 6C](#) and [6D](#)).

As the major surrogate for GC Tfh cell activity, c-Tfh cells would be expected to represent an activated memory subset within peripheral blood. To investigate this, we examined an activated population hypothesized to egress from LNs post vaccination, CD38+ ICOS+ c-Tfh ([Herati et al., 2017](#)). However, we observed no significant difference in the frequency of CD38+ ICOS+ c-Tfh cells between baseline and day 5 postvaccination ([Figure S5D](#)). Further, no correlation was observed between frequency of CD38+ ICOS+ c-Tfh cells and CD38+ ICOS+ GC Tfh cells from draining LNs was observed at baseline ([Figure 6E](#)) or day 5 ([Figure 6F](#)) or with CD38+ ICOS+ GC Tfh cells from contralateral LNs at baseline or day 5 ([Figures S5E](#) and [S5F](#)). Similarly, there was no correlation between the frequency of CD38+ ICOS+ c-Tfh and CD38+ ICOS+ Pre-Tfh from draining LN ([Figure 6G](#)). However, a moderate positive correlation was observed between these two subsets at day 5 postvaccination ([Figure 6H](#)). These data highlight the potential limitations of using c-Tfh cells as a surrogate marker and the need to directly assess immune responses in tissues where they are staged.

Expansion of influenza-specific CD4+ T cells in peripheral blood five days postvaccination

Antigen specificity is an important parameter of protective vaccine evaluation as it influences the functionality of the T cell response including, perhaps crucially, the Tfh cell response ([Sant et al., 2018](#), [Dipiiazza et al., 2016](#)). Influenza-specific responses postvaccination were measured using the OX40 T cell assay ([Zaunders et al., 2009](#)). When the frequencies of CD25+ CD134+ T cells were compared between baseline and day 5, no difference was observed in the positive control SEB stimulation cultures ([Figure 7A](#)). However, frequency of influenza-specific CD4+ T cells were significantly increased in peripheral blood by day 5

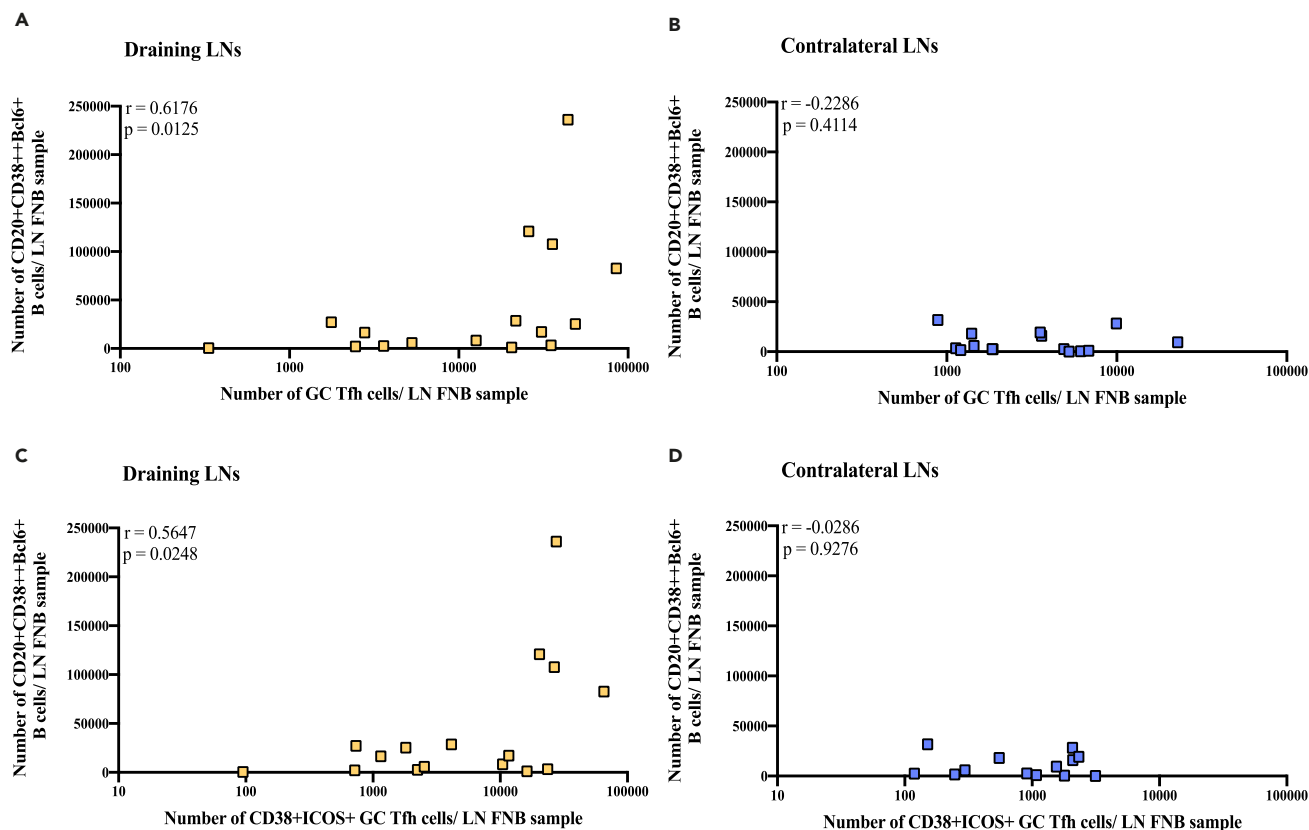


Figure 4. Correlation of absolute GC B cell number with GC Tfh cell number and CD38+ICOS+GC Tfh cell number in draining LNs at day 5

(A) Significant positive correlation between absolute number of GC B cells and GC Tfh cells in draining LNs at day 5.

(B) Relationship between GC Tfh cells and GC B cells in contralateral LNs at day 5.

(C) Significant positive correlation between absolute number of GC B cells and CD38+ ICOS+ GC Tfh cells in draining LNs at day 5.

(D) Relationship between CD38+ ICOS+ GC Tfh cells and GC B cells in contralateral LNs at day 5. All correlations were calculated using a Spearman's correlation.

when stimulated with influenza A peptides (Figure 7B) or influenza A viral lysate (Figure 7C). No correlation was observed between frequency of influenza-specific CD25 + CD134 + T cells in the periphery and the frequency of Tfh cells from draining LNs at baseline (Figure 7D) or day 5 (Figure 7E). In this study, we saw no significant difference in peripheral antigen specific c-Tfh between baseline and day 5 (Figure 7F). We also observed no significant difference in antigen specific Treg cells between baseline and day 5 (Figure 7G). Although antigen-specific T cell responses were detectable as early as 5 days postvaccination, the lack of correlation with GC Tfh cells from LNs suggests day 5 is too early to detect the peak immune response in the periphery.

DISCUSSION

The difficulty of accessing human secondary lymphoid tissues, the site of generation and coordination of adaptive humoral immune responses, has limited the direct interrogation of human immune responses. This study sought to examine the early changes in cellular profiles relative to a prevaccination timepoint, in particular GC Tfh cells, within the draining LNs of previously immunized healthy human volunteers receiving seasonal influenza vaccination. We show an expansion in the absolute number of GC Tfh cells postvaccination which is restricted to the draining LNs. Although no significant difference in GC B cell numbers was observed between baseline and day 5, the number of GC B cells at day 5 in draining LNs was significantly greater than in contralateral LNs. Although initially an unexpected result, the contemporaneous contralateral LN controls for systemic changes that could affect the host that may not be recognized or predicted. In addition, vaccination has a systemic effect on the host, as well as the draining LN in particular. Using baseline as the only control would rely solely on the host in a prevaccination state,

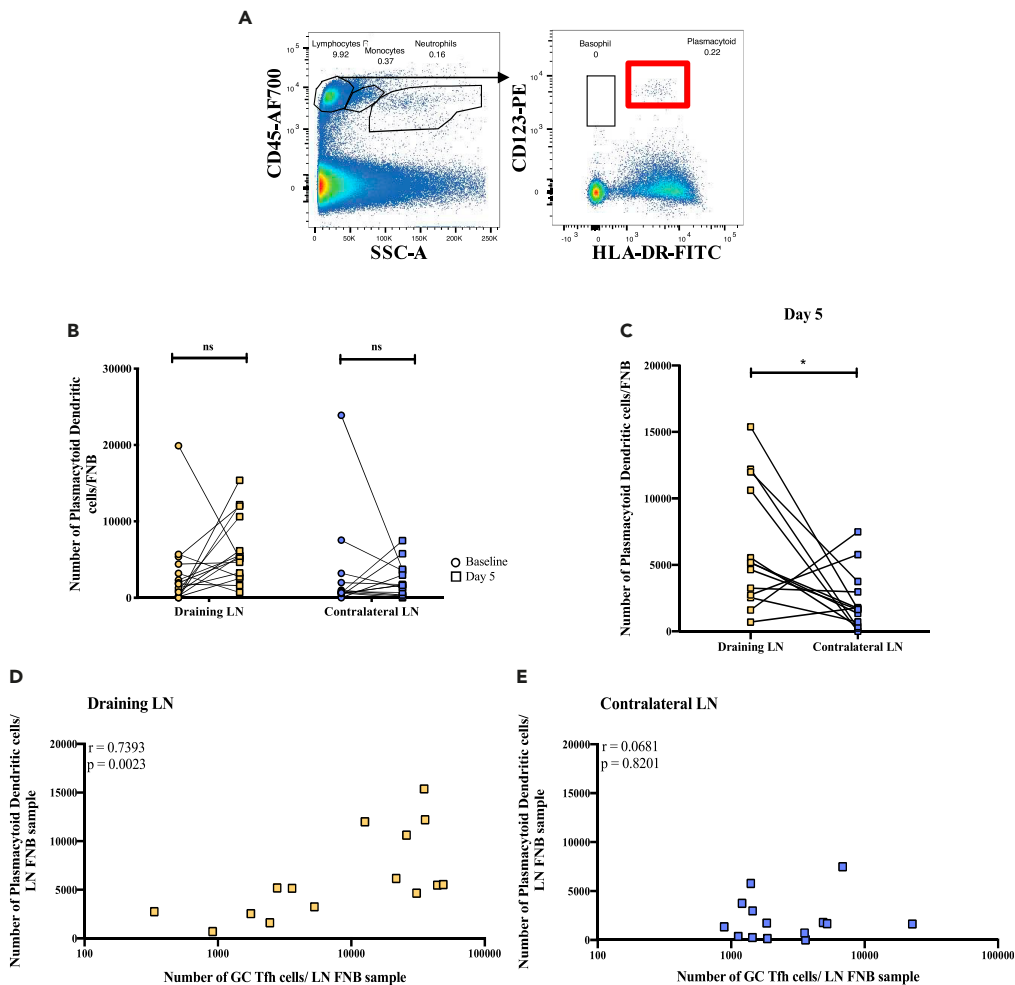


Figure 5. Plasmacytoid Dendritic cells expand in draining LNs

(A) Representative flow cytometry plot of pDC gating. SSC-A versus CD45 was used to identify CD45+ Lymphocytes, followed by CD123 versus HLA-DR to identify CD123+HLA-DR+ pDCs.

(B) No significant difference in absolute number of pDCs between baseline and day 5 was observed in draining or contralateral LNs.

(C) Absolute number of pDCs were significantly higher in draining LNs compared to contralateral LNs at day 5 postvaccination, *, $p < 0.05$ (Wilcoxon signed rank).

(D) Significant positive correlation between absolute number of pDCs and GC Tfh cells in draining LNs at day 5. (E)

Relationship between CD38+ ICOS+ Tfh cells and GC B cells in contralateral LNs at day 5. All correlations were calculated using a Spearman's correlation. Yellow = draining LNs; Blue = contralateral LNs. See also [Figure S4](#).

whereas the contemporaneous LN at day 5 is an internal control to the host that accounts for any unforeseen or unrealized biases introduced by the vaccination. The expanded GC Tfh population in the draining LNs is significantly more activated and potentially motile, as determined by expression levels of CD38 and ICOS, measured by MFI. Perhaps the most unexpected implication this work will have on future studies is the unique method of quantification of GC Tfh cell populations using absolute cell number, revealing key biological insights into the early changes in cellular profiles of the GC postvaccination that were previously unable to be detected (Kil et al., 2019).

CD38 is widely accepted as a marker of activation in T cells and is upregulated in the early stages of the immune response (Piedra-Quintero et al., 2020; Zaunders et al., 2005, 2006). CD38, a surface glycoprotein and cyclic ADP ribose hydrolase, is thought to facilitate costimulatory interactions between activated B cells and helper T cells (Manjarrez-Orduno et al., 2007), and therefore was of particular interest in this study. Importantly, GC Tfh activation, as measured by CD38 surface expression, was significantly higher at day 5

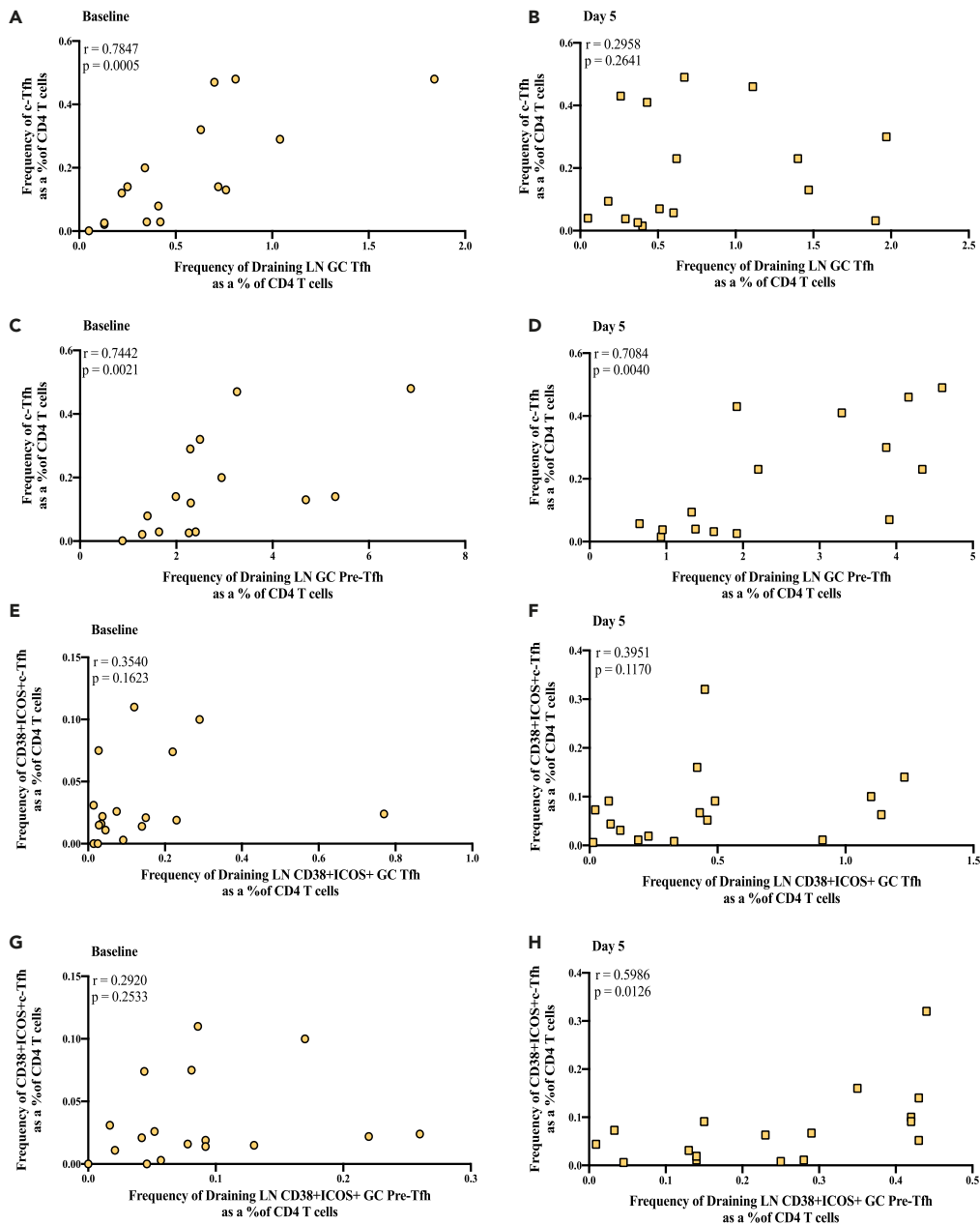


Figure 6. Relationship between c-Tfh in peripheral blood and GC Tfh cells

(A) Significant positive correlation between frequency of c-Tfh cells and frequency of GC Tfh cells in draining LNs at baseline.
 (B) No correlation between frequency of c-Tfh cells and frequency of GC Tfh cells in draining LNs at day 5.
 (C) Significant positive correlation between frequency of c-Tfh cells and frequency of Pre-Tfh cells in draining LNs at baseline.
 (D) Significant positive correlation between frequency of c-Tfh cells and frequency of Pre-Tfh cells in draining LNs at day 5.
 (E) Relationship between CD38+ ICOS+ c-Tfh and CD38+ ICOS+ GC Tfh from draining LNs at baseline.
 (F) Relationship between CD38+ ICOS+ c-Tfh and CD38+ ICOS+ GC Tfh from draining LNs at day 5.
 (G) Relationship between CD38+ ICOS+ c-Tfh and CD38+ ICOS+ Pre-Tfh from draining LNs at baseline.
 (H) Significant moderate correlation between frequency of CD38+ ICOS+ c-Tfh and CD38+ ICOS+ Pre-Tfh from draining LNs at day 5. All correlations were calculated using a Spearman's correlation. Yellow = draining LNs; Blue = contralateral LNs; circles = baseline; squares = day 5. See also Figure S5.

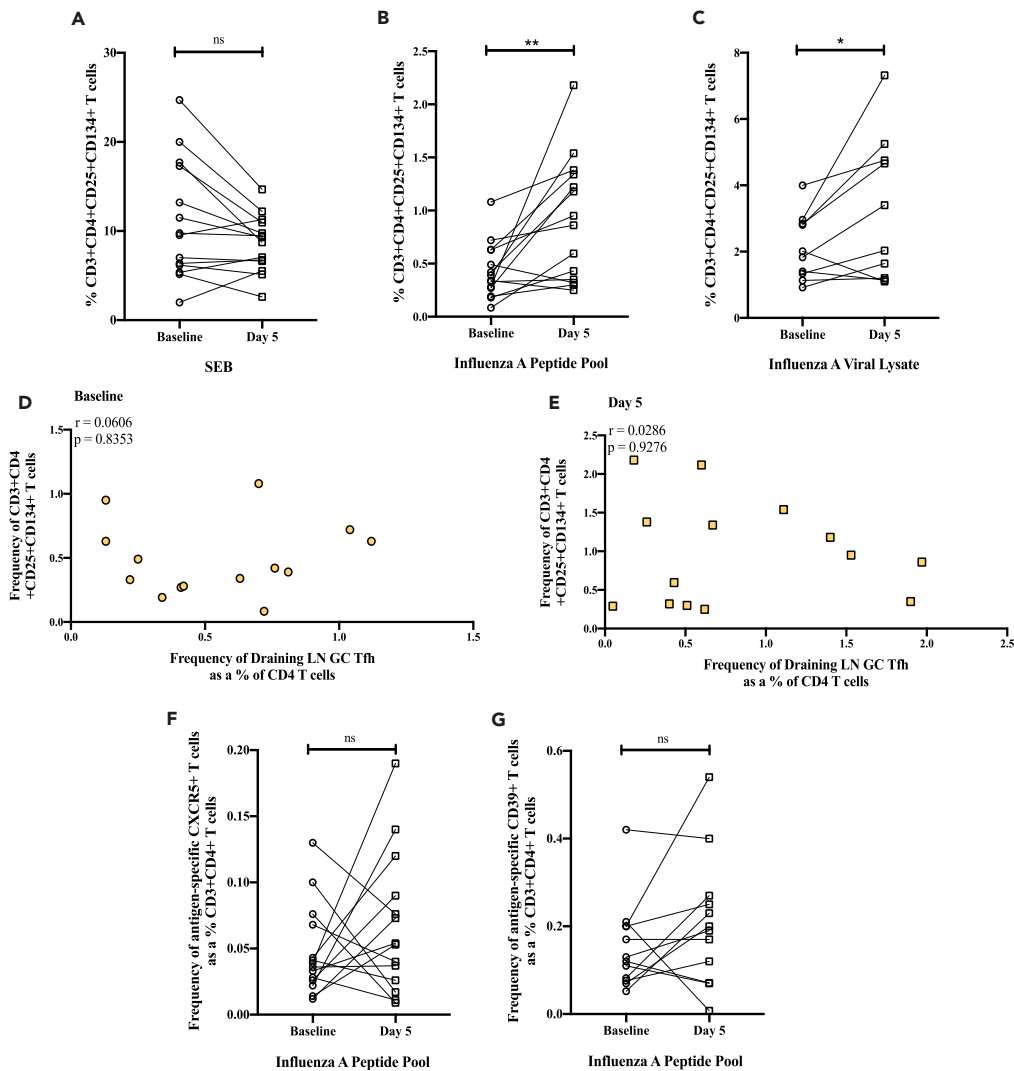


Figure 7. Frequency of antigen-specific CD4 T cells and their relationship to GC Tfh cells

(A) No significant difference in the frequency of SEB antigen specific CD4 T cells.
 (B) Frequency of influenza antigen specific CD4 T cells was significantly higher than baseline at day 5 postvaccination when stimulated with Influenza A peptides.
 (C) Frequency of influenza antigen specific CD4 T cells was significantly higher at day 5 postvaccination in cultures stimulated with Influenza A viral lysate.
 (D) No correlation between influenza antigen specific CD4 T cells from peripheral whole blood and GC Tfh cells from draining LNs at baseline.
 (E) No correlation between influenza antigen specific CD4 T cells from peripheral whole blood and GC Tfh cells from draining LNs at day 5.
 (F) No significant difference in the frequency of influenza antigen specific CXCR5+ c-Tfh between baseline and day 5 postvaccination.
 (G) No significant difference in the frequency of influenza antigen specific CD39+ Treg between baseline and day 5 postvaccination. ns, non-significant; * $p < 0.05$; ** $p < 0.01$. Comparisons between baseline and day 5 cell frequencies were calculated using a Wilcoxon signed rank. Correlations between cell frequencies were assessed using a Spearman's correlation. Yellow = draining LNs; circles = baseline; squares = day 5.

postvaccination in the draining LN compared to baseline, demonstrating that early after boosting vaccination, lymphocyte activation occurs exclusively in the draining LNs.

Pre-Tfh and Tfh cell motility within the LN is dependent on cytoskeletal remodeling induced by ICOS mediated PI3K activation (Gigoux et al., 2009; Kang et al., 2013). Once inside the GC, ICOS expression is known

to be a key inducer of Tfh cell differentiation and essential for their interactions with GC B cells during the GC reaction (Leavenworth et al., 2015; Choi et al., 2011; Mcadam et al., 2001; Akiba et al., 2005). We found that draining LN GC Tfh and Pre-Tfh cells had significantly higher ICOS expression at day 5 compared to baseline, and also compared to the same cells from contralateral LNs. Increased expression of ICOS on Pre-Tfh cells suggests this population is highly motile and potentially represents a distinct subset in the early stages of differentiation into GC Tfh cells. Taken together, these results are the first to demonstrate selective expansion and activation of draining LN GC Tfh cells and Pre-Tfh cells that suggests the GC reaction occurs as early as 5 days postvaccination in humans. The observation that the immune response to vaccination is restricted to the draining LN was further supported by the correlation of GC B cell number with GC Tfh cell number in only draining LNs.

This study demonstrates that expansion of CD38+ ICOS+ GC Tfh cells and CD38+ ICOS+ Pre-Tfh cells occurs in human draining LNs within days of vaccination. Further, the data shows for the first time in humans, increases in CD38 + Ki67+ GC Tfh cells and CD38+ Ki67+ Pre-Tfh cells occur exclusively in the draining LNs, suggesting active proliferation of these crucial immune cells postvaccination. Although there was no expansion in absolute number of Pre-Tfh cells postvaccination, this population expresses Tfh transcription factor Bcl6 and contained a significantly expanded subpopulation of highly activated, proliferating cells. These results could suggest that these highly activated Pre-Tfh cells are migrating to the GC and differentiating into GC Tfh cells to ultimately contribute to the expansion of the GC Tfh cell population postvaccination.

Previous work has suggested that CD38+ ICOS+ Tfh cells egress from the LN and enter the circulation as c-Tfh seven days postvaccination, which include a population of antigen-specific cells (Herati et al., 2017). It is also possible that these CD38+ ICOS+ GC Tfh expand within the draining LNs and give rise to antigen-specific cells that can enter the periphery forming a memory population. However, as we observed no relationship between CD38+ ICOS+ GC Tfh and CD38+ ICOS+ c-Tfh five days postvaccination, it is likely that day 5 may be too early to detect GC Tfh that have entered the periphery and further studies are underway. Although there has been much discussion about the role of vaccination site in immune responses (Cook et al., 2006; Mark et al., 1999), these results present the first snapshot that early Tfh cell activation and GC B cell responses to vaccination within the LN system are localized to LNs draining the site of vaccination. Correlation of GC B cells with ICOS+ CD38+ GC Tfh cells from draining LNs further supports this spatial restriction of the immune response. Importantly, these results demonstrate both quantitative and qualitative changes in crucial immune cell subsets postvaccination.

The presence of a circulating Tfh-like population found in peripheral blood is now widely accepted in the literature and the extensive study of this intriguing population has highlighted the necessity of a surrogate population for *bona fide* GC Tfh cells. Indeed, sampling of human thoracic duct has identified CXCR5^{high} PD-1^{high} Tfh cells that shared phenotypic and transcriptional similarities with GC Tfh cells and may be intermediate between Tfh cells in blood and secondary lymphoid tissues (Vella et al., 2019). Previous studies have demonstrated expansion of c-Tfh cells seven days post vaccination (Koutsakos et al., 2018), including an antigen-specific c-Tfh population in response to influenza vaccination (Herati et al., 2017; Heit et al., 2017), COVID-19 infection (Juno et al., 2020), and HIV infection (Niessl et al., 2020; Claireaux et al., 2018). However, we saw no increase in frequency of c-Tfh cells or of the CD38+ ICOS+ subset of c-Tfh cells at day 5 postvaccination. Although previous studies have established a clonal and transcriptional relationship between Tfh cells from secondary lymphoid organs and c-Tfh in peripheral blood (Heit et al., 2017; Hill et al., 2019; Brenna et al., 2020), here we observed no relationship between draining LN GC Tfh cells and c-Tfh at day 5 postvaccination. Another possible origin of the c-Tfh population and the highly activated CD38+ ICOS+ subsets is the CD38+ ICOS+ Pre-Tfh population as suggested by the moderately positive correlation between these two populations. It is possible that the highly activated GC Tfh population remains within the LN, and the Pre-Tfh cell population gives rise to both early GC Tfh and c-Tfh upon activation; however, further investigation is required. Therefore, this study illustrates that critical changes in cellular profiles and interactions in early responses to vaccination occur exclusively within the draining LNs, posing the following question: are c-Tfh cells the most appropriate surrogate marker for GC Tfh cells in studying early immune responses to vaccination?

We saw a significant increase in antigen-specific CD4+ T cells in peripheral blood, an accepted marker of immune responses to vaccination (Zaunders et al., 2009; Cook et al., 2020). However, the frequency of this

antigen-specific CD4⁺ T cell population did not correlate with the frequency of LN GC Tfh cells in draining, or contralateral, LNs at day 5. Within the antigen-specific CD4⁺ T cell population, we identified a subpopulation of antigen-specific c-Tfh cells but saw no significant difference in their frequency postvaccination. Although antigen-specific CD4⁺ T cells are expanded and antigen-specific c-Tfh are detectable 5 days postvaccination, the lack of relationship between these circulating subsets and draining LN GC Tfh cells, supports the conclusion that 5 days postvaccination is too early to observe the potential entry of a subset of Tfh into the circulation. It is possible the expansion of antigen-specific cells in the periphery could occur in sequential waves. Firstly, the expansion of antigen-specific CD4⁺ T cells detectable at day 5 postvaccination, followed by a later expansion of antigen-specific c-Tfh cells possibly detectable at a later time point. This potential difference in circulatory patterns could be indicative of different circulation, phenotypes, and roles for these two subpopulations and warrants further investigation.

The ability to access human lymphoid tissue comes with a number of both ethical and practical obstacles. Even with the use of ultrasound guided LN FNBs, radiologists must identify a safely accessible LN within the axillary region where nodes are typically small, located relatively deep in the tissues and may be difficult to approach because of the vasculature or the brachial plexus. Once accessed the needle must successfully pierce the LN capsule to sample the inner cortex. The sampling of the cortex, determined by the detection of appropriate subsets of lymph node resident lymphocytes, and the absence of blood contamination, identified as the absence of NK cell, neutrophil and monocyte cell populations, were our primary indicators of success. Lymph node composition, measured by lymphocyte subset frequencies, was consistent with previous sacrifice studies and was a further indicator of success (Xu et al., 2013a). Despite a large spread in total lymphocyte yields, from 6.8×10^3 to 12.2×10^6 cells, lymphocyte numbers were sufficient for downstream analysis.

Although LN FNBs are an established technique for detection of neoplastic cells in clinical settings, our ability to identify multiple normal cellular populations; including pDCs, GC Tfr, Follicular Tfr, T cell zone Tfr, GC B cells, and GC Tfh cells and their precursors, Pre-Tfh cells, as well as monitoring qualitative changes in the activation state of these subsets following an *in vivo* stimulus, extends previous findings confirming that FNBs can be uniquely adopted in the research setting to probe, identify, and analyze critical immune cells within secondary lymphoid tissues in longitudinal studies (Hey-Nguyen et al., 2017; Turner et al., 2020; Havenar-Daughton et al., 2020). This expansion of our previous work on inguinal nodes, to longitudinal sampling of axillary nodes postvaccination in the absence of blood contamination, high sampling success rate, and lack of significant adverse complications or infections, solidifies this technique as a safe, reproducible, and viable solution to the physiological and ethical obstacles faced by researchers when studying immune responses *in vivo* in humans.

This study demonstrates FNBs can access lymph node resident cells, such as pDCs which are of particular interest as they traffic to secondary lymphoid tissues in response to inflammation where they can activate T cells and, in the context of HIV, contribute to chronicity and formation of the viral reservoir through dysregulated activation and IFN type-1 production (Cella et al., 2000; Swiecki and Colonna, 2015). Here, we demonstrate that the FNB technique is able to detect rare cell populations such as pDCs, which could be of significant interest in future studies. The FNB technique is particularly applicable to studies investigating the susceptibility of Tfh and Pre-Tfh cells to HIV infection and their likely role in formation and maintenance of the HIV viral reservoir (Xu et al., 2017; Zaunders et al., 2017; Banga et al., 2016).

Limitations of the study

Despite the use of sophisticated radiological techniques to enumerate follicular responses in LN, this study does have limitations. As previously discussed, the small size of axillary LNs and their close proximity to a number of vessels and the brachial plexus presents a significant obstacle to even an expert radiographer skilled in the technique. Despite preexisting expertise derived from accessing pathologically involved nodes, a training effect was observed in the ability to successfully access the axillary nodes in healthy volunteers. Although a LN may be successfully sampled, we are unable to determine the exact location within the LN of the sampling or how many passes of the needle into the lymph node were successful. However, we have previously shown that the proportions of cell populations obtained by FNB are representative of the populations within the LN in both health and disease (Xu et al., 2013a). This study was also restricted by samples without matching pairs (either baseline matched with day 5 or draining matched with contralateral), which were excluded from analysis. A second limitation was the number of cells we obtained.

Although enough cells were recovered for sufficient phenotypic analysis, further work is required to allow reproducible functional studies to be performed on these samples with low cell number and the highly activated state of the cells of interest with their propensity to apoptosis once removed from their microenvironment. A further limitation of this work is the lack of extended sampling timepoints which would provide interesting and valuable data about the longitudinal profile of the humoral immune response, both within the LN and in the periphery, and the expansion of the c-Tfh cell population and their relationship to the GC response.

Nevertheless, these results are, to our knowledge, the first to quantify the selective activation and proliferative capacity of GC Tfh cells and other critical immune cell subsets postvaccination in human draining axillary LNs. Through sequential sampling, we show that draining LN GC Tfh and Pre-Tfh cells become enabled for migration and upregulate receptors critical for Tfh cell differentiation that also facilitate cellular interactions essential during GC reactions. Contrary to previous studies (Kil et al., 2019), expansion of the GC Tfh cell population was detected by quantifying absolute cell number rather than using the standard measurement of the frequency of the population, providing key biological insight into the LN. These consistent results provide significant justification and opportunities for further interrogation of LN Tfh cells and their potential to form antigen specific populations in both LNs and c-Tfh populations to optimize immune responses to vaccination.

STAR★METHODS

Detailed methods are provided in the online version of this paper and include the following:

- KEY RESOURCES TABLE
- RESOURCE AVAILABILITY
 - Lead contact
 - Materials availability
 - Data and code availability
- EXPERIMENTAL MODEL AND SUBJECT DETAILS
 - Study participants
 - Lymph node fine needle biopsies
- METHOD DETAILS
 - Flow cytometry
 - Functional assays
 - Quality control of LN FNB
- QUANTIFICATION AND STATISTICAL ANALYSIS
 - Statistics

SUPPLEMENTAL INFORMATION

Supplemental information can be found online at <https://doi.org/10.1016/j.isci.2021.103656>.

ACKNOWLEDGMENTS

The authors would like to acknowledge the incredible and invaluable administrative and laboratory support of Trever Dougherty and Katherine Marks, respectively. Further thanks must be extended to Dr. Emma Johansson-Beves at the Biological Resources Imaging Laboratory at Mark Wainwright Analytical Centre, UNSW. Funding: This work was supported by a University of New South Wales Research Training Program Scholarship (RSAP1000) (H.L.), a National Health and Medical Research Council Career Development Fellowship 1067590 (V.V.), a National Health and Medical Research Council Senior Research Fellowship 1155678 (T.G.P), a National Health and Medical Research Council Program grant 1149990 (A.D.K. and C.M.M.) and a St Vincent's Clinic Foundation Grant (2018).

AUTHOR CONTRIBUTIONS

Conceptualization: JZ, ADK, CMM. Experimental design: JZ, ADK, CMM, HL, TP. Sample collection: AH, SO, BM, CC, ME, BF, KO. Methodology-experimental: HL, MM, CMM, AH, YX. Methodology-data analysis: HL, CMM. Methodology-statistical analysis and visualization: HL. Statistical advice: VV. Study oversight and coordination: DC, CMM. Writing-original draft: HL. Writing-review and editing: ADK, CMM, JZ, VV, DC, TP, HL.

DECLARATIONS OF INTERESTS

The authors declare no competing conflicts of interest.

INCLUSION AND DIVERSITY

We worked to ensure gender balance in the recruitment of human subjects.

Received: August 26, 2021

Revised: November 22, 2021

Accepted: December 14, 2021

Published: January 21, 2022

REFERENCES

- Akiba, H., Takeda, K., Kojima, Y., Usui, Y., Harada, N., Yamazaki, T., MA, J., Tezuka, K., Yagita, H., and Okumura, K. (2005). The role of ICOS in the CXCR5+ follicular B helper T cell maintenance in vivo. *J. Immunol.* 175, 2340–2348.
- Banga, R., Procopio, F.A., Noto, A., Pollakis, G., Cavassini, M., Ohmiti, K., Corpataux, J.M., DE Leval, L., Pantaleo, G., and Perreau, M. (2016). PD-1(+) and follicular helper T cells are responsible for persistent HIV-1 transcription in treated aviremic individuals. *Nat. Med.* 22, 754–761.
- Bentebibel, S.E., Khurana, S., Schmitt, N., Kurup, P., Mueller, C., Obermoser, G., Palucka, A.K., Albrecht, R.A., Garcia-Sastre, A., Golding, H., and Ueno, H. (2016). ICOS(+)PD-1(+)CXCR3(+) T follicular helper cells contribute to the generation of high-avidity antibodies following influenza vaccination. *Sci. Rep.* 6, 26494.
- Bentebibel, S.E., Lopez, S., Obermoser, G., Schmitt, N., Mueller, C., Harrod, C., Flano, E., Mejias, A., Albrecht, R.A., Blankenship, D., et al. (2013). Induction of ICOS+CXCR3+CXCR5+ TH cells correlates with antibody responses to influenza vaccination. *Sci. Transl. Med.* 5, 176ra32.
- Brenna, E., Davydov, A.N., Ladell, K., McLaren, J.E., Bonaiuto, P., Metsger, M., Ramsden, J.D., Gilbert, S.C., Lambe, T., Price, D.A., et al. (2020). CD4(+) T follicular helper cells in human tonsils and blood are clonally convergent but divergent from non-Tfh CD4(+) cells. *Cell Rep.* 30, 137–152.e5.
- Cella, M., Facchetti, F., Lanzavecchia, A., and Colonna, M. (2000). Plasmacytoid dendritic cells activated by influenza virus and CD40L drive a potent TH1 polarization. *Nat. Immunol.* 1, 305–310.
- Choi, Y.S., Kageyama, R., Eto, D., Escobar, T.C., Johnston, R.J., Monticelli, L., Lao, C., and Crotty, S. (2011). ICOS receptor instructs T follicular helper cell versus effector cell differentiation via induction of the transcriptional repressor Bcl6. *Immunity* 34, 932–946.
- Claireaux, M., Galperin, M., Benati, D., Nouel, A., Mukhopadhyay, M., Klingler, J., De Truchis, P., Zucman, D., Houdou, S., Boufassa, F., et al. (2018). A high frequency of HIV-specific circulating follicular helper T cells is associated with preserved memory B cell responses in HIV controllers. *mBio* 9. <https://doi.org/10.1128/mBio.00317-18>.
- Cook, I.F., Barr, I., Hartel, G., Pond, D., and Hampson, A.W. (2006). Reactogenicity and immunogenicity of an inactivated influenza vaccine administered by intramuscular or subcutaneous injection in elderly adults. *Vaccine* 24, 2395–2402.
- Cook, L., Munier, C.M.L., Seddiki, N., Hardy, M.Y., Anderson, R.P., Zunders, J., Tye-Din, J.A., Kelleher, A.D., and Van Bockel, D. (2020). Circulating gluten-specific, but not CMV-specific, CD39(+) regulatory T cells have an oligoclonal TCR repertoire. *Clin. Transl. Immunol.* 9, e1096.
- Crotty, S. (2014). T follicular helper cell differentiation, function, and roles in disease. *Immunity* 41, 529–542.
- Dhaeze, T., Peelen, E., Hombrouck, A., Peeters, L., Van Wijmeersch, B., Lemkens, N., Lemkens, P., Somers, V., Lucas, S., Broux, B., et al. (2015). Circulating follicular regulatory T cells are defective in multiple sclerosis. *J. Immunol.* 195, 832–840.
- Dipiazza, A., Richards, K.A., Knowlden, Z.A., Nayak, J.L., and Sant, A.J. (2016). The role of CD4 T cell memory in generating protective immunity to novel and potentially pandemic strains of influenza. *Front. Immunol.* 7, 10.
- Fazilleau, N., Mark, L., Mcheyzer-Williams, L.J., and Mcheyzer-Williams, M.G. (2009). Follicular helper T cells: lineage and location. *Immunity* 30, 324–335.
- Fazilleau, N., Mcheyzer-Williams, L.J., and Mcheyzer-Williams, M.G. (2007). Local development of effector and memory T helper cells. *Curr. Opin. Immunol.* 19, 259–267.
- Fonseca, V.R., Agua-Doce, A., Maceiras, A.R., Pierson, W., Ribeiro, F., Romao, V.C., Pires, A.R., Da Silva, S.L., Fonseca, J.E., Sousa, A.E., et al. (2017). Human blood Tfr cells are indicators of ongoing humoral activity not fully licensed with suppressive function. *Sci. Immunol.* 2, eaan1487.
- Gigoux, M., Shang, J., Pak, Y., Xu, M., Choe, J., Mak, T.W., and Suh, W.K. (2009). Inducible costimulator promotes helper T-cell differentiation through phosphoinositide 3-kinase. *Proc. Natl. Acad. Sci. U S A* 106, 20371–20376.
- Harker, J.A., Lewis, G.M., Mack, L., and Zuniga, E.I. (2011). Late interleukin-6 escalates T follicular helper cell responses and controls a chronic viral infection. *Science* 334, 825–829.
- Havenar-Daughton, C., Carnathan, D.G., Torrents De La Pena, A., Pauthner, M., Briney, B., Reiss, S.M., Wood, J.S., Kaushik, K., Van Gils, M.J., Rosales, S.L., et al. (2016). Direct probing of germinal center responses reveals immunological features and bottlenecks for neutralizing antibody responses to HIV env Trimer. *Cell Rep.* 17, 2195–2209.
- Havenar-Daughton, C., Newton, I.G., Zare, S.Y., Reiss, S.M., Schwan, B., Suh, M.J., Hasteh, F., Levi, G., and Crotty, S. (2020). Normal human lymph node T follicular helper cells and germinal center B cells accessed via fine needle aspirations. *J. Immunol. Methods* 479, 112746.
- Heit, A., Schmitz, F., Gerdtts, S., Flach, B., Moore, M.S., Perkins, J.A., Robins, H.S., Aderem, A., Spearman, P., Tomaras, G.D., et al. (2017). Vaccination establishes clonal relatives of germinal center T cells in the blood of humans. *J. Exp. Med.* 214, 2139–2152.
- Herati, R.S., Muselman, A., Vella, L., Bengsch, B., Parkhouse, K., Del Alcazar, D., Kotzin, J., Doyle, S.A., Tebas, P., Hensley, S.E., et al. (2017). Successive annual influenza vaccination induces a recurrent oligoclonotypic memory response in circulating T follicular helper cells. *Sci. Immunol.* 2, eaag2152.
- Herati, R.S., Reuter, M.A., Dolfi, D.V., Mansfield, K.D., Aung, H., Badwan, O.Z., Kurupati, R.K., Kannan, S., Ertl, H., Schmadler, K.E., et al. (2014). Circulating CXCR5+PD-1+ response predicts influenza vaccine antibody responses in young adults but not elderly adults. *J. Immunol.* 193, 3528–3537.
- Hey-Nguyen, W.J., Xu, Y., Pearson, C.F., Bailey, M., Suzuki, K., Tantau, R., Obeid, S., Milner, B., Field, A., Carr, A., et al. (2017). Quantification of residual germinal center activity and HIV-1 DNA and RNA levels using fine needle biopsies of lymph nodes during antiretroviral therapy. *AIDS Res. Hum. Retroviruses* 33, 648–657.
- Hill, D.L., Pierson, W., Bolland, D.J., Mkindi, C., Carr, E.J., Wang, J., Houard, S., Wingett, S.W., Audran, R., Wallin, E.F., et al. (2019). The adjuvant GLA-SE promotes human Tfh cell expansion and emergence of public TCRbeta clonotypes. *J. Exp. Med.* 216, 1857–1873.
- Huang, Y., Chen, Z., Wang, H., Ba, X., Shen, P., Lin, W., Wang, Y., Qin, K., Huang, Y., and Tu, S. (2020). Follicular regulatory T cells: a novel target for immunotherapy? *Clin. Transl. Immunol.* 9, e1106.
- Inoue, T., Moran, I., Shinnakasu, R., Phan, T.G., and Kurosaki, T. (2018). Generation of memory B

- cells and their reactivation. *Immunol. Rev.* **283**, 138–149.
- Juno, J.A., Tan, H.X., Lee, W.S., Reynaldi, A., Kelly, H.G., Wragg, K., Esterbauer, R., Kent, H.E., Batten, C.J., Mordant, F.L., et al. (2020). Humoral and circulating follicular helper T cell responses in recovered patients with COVID-19. *Nat. Med.* **26**, 1428–1434.
- Kang, S.G., Liu, W.H., Lu, P., Jin, H.Y., Lim, H.W., Shepherd, J., Fremgen, D., Verdin, E., Oldstone, M.B., Qi, H., et al. (2013). MicroRNAs of the miR-17 approximately 92 family are critical regulators of T(FH) differentiation. *Nat. Immunol.* **14**, 849–857.
- Kil, L.P., Vaneman, J., Van Der Lubbe, J.E.M., Czapska-Casey, D., Tolboom, J., Roozendaal, R., Zahn, R.C., Kuipers, H., and Solfrosi, L. (2019). Restrained expansion of the recall germinal center response as biomarker of protection for influenza vaccination in mice. *PLoS One* **14**, e0225063.
- Koutsakos, M., Wheatley, A.K., Loh, L., Clemens, E.B., Sant, S., Nussing, S., Fox, A., Chung, A.W., Laurie, K.L., Hurt, A.C., et al. (2018). Circulating TFH cells, serological memory, and tissue compartmentalization shape human influenza-specific B cell immunity. *Sci. Transl. Med.* **10**. <https://doi.org/10.1126/scitranslmed.aan8405>.
- Krammer, F., Smith, G.J.D., Fouchier, R.A.M., Peiris, M., Kedzierska, K., Doherty, P.C., Palese, P., Shaw, M.L., Treanor, J., Webster, R.G., and Garcia-Sastre, A. (2018). Influenza. *Nat. Rev. Dis. Primers* **4**, 3.
- Leavenworth, J.W., Verbinen, B., Yin, J., Huang, H., and Cantor, H. (2015). A p85alpha-osteopontin axis couples the receptor ICOS to sustained Bcl-6 expression by follicular helper and regulatory T cells. *Nat. Immunol.* **16**, 96–106.
- Locci, M., Havenar-Daughton, C., Landais, E., Wu, J., Kroenke, M.A., Arlehamn, C.L., Su, L.F., Cubas, R., Davis, M.M., Sette, A., et al. (2013). Human circulating PD-1+CXCR3-CXCR5+ memory Tfh cells are highly functional and correlate with broadly neutralizing HIV antibody responses. *Immunity* **39**, 758–769.
- Lopez, M.J., Seyed-Razavi, Y., Yamaguchi, T., Ortiz, G., Sendra, V.G., Harris, D.L., Jamali, A., and Hamrah, P. (2020). Multiphoton intravital microscopy of mandibular draining lymph nodes: a mouse model to study corneal immune responses. *Front. Immunol.* **11**. <https://doi.org/10.3389/fimmu.2020.00039>.
- Ma, C.S., and Phan, T.G. (2017). Here, there and everywhere: T follicular helper cells on the move. *Immunology* **152**, 382–387.
- Manjarrez-Orduno, N., Moreno-Garcia, M.E., Fink, K., and Santos-Argumedo, L. (2007). CD38 cross-linking enhances TLR-induced B cell proliferation but decreases IgM plasma cell differentiation. *Eur. J. Immunol.* **37**, 358–367.
- Mark, A., Carlsson, R.M., and Granstrom, M. (1999). Subcutaneous versus intramuscular injection for booster DT vaccination of adolescents. *Vaccine* **17**, 2067–2072.
- Mcadam, A.J., Greenwald, R.J., Levin, M.A., Chernova, T., Malenkovich, N., Ling, V., Freeman, G.J., and Sharpe, A.H. (2001). ICOS is critical for CD40-mediated antibody class switching. *Nature* **409**, 102–105.
- Miller, M.J., Wei, S.H., Parker, I., and Cahalan, M.D. (2002). Two-photon imaging of lymphocyte motility and antigen response in intact lymph node. *Science* **296**, 1869–1873.
- Moran, I., Nguyen, A., Khoo, W.H., Butt, D., Bourne, K., Young, C., Hermes, J.R., Biro, M., Gracie, G., Ma, C.S., et al. (2018). Memory B cells are reactivated in subcapsular proliferative foci of lymph nodes. *Nat. Commun.* **9**, 3372.
- Murali, R., Thompson, J.F., Uren, R.F., and Scolyer, R.A. (2010). Fine-needle biopsy of metastatic melanoma: clinical use and new applications. *Lancet Oncol.* **11**, 391–400.
- Niessl, J., Baxter, A.E., Morou, A., Brunet-Ratnasingham, E., Sannier, G., Gendron-Lepage, G., Richard, J., Delgado, G.G., Brassard, N., Turcotte, I., et al. (2020). Persistent expansion and Th1-like skewing of HIV-specific circulating T follicular helper cells during antiretroviral therapy. *EBioMedicine* **54**, 102727.
- Perreau, M., Savoye, A.L., De Crignis, E., Corpataux, J.M., Cubas, R., Haddad, E.K., De Leval, L., Graziosi, C., and Pantaleo, G. (2013). Follicular helper T cells serve as the major CD4 T cell compartment for HIV-1 infection, replication, and production. *J. Exp. Med.* **210**, 143–156.
- Piedra-Quintero, Z.L., Wilson, Z., Nava, P., and Guerau-De-Arellano, M. (2020). CD38: an immunomodulatory molecule in inflammation and autoimmunity. *Front Immunol* **11**, 597959.
- Pilkinton, M.A., Nicholas, K.J., Warren, C.M., Smith, R.M., Yoder, S.M., Talbot, H.K., and Kalams, S.A. (2017). Greater activation of peripheral T follicular helper cells following high dose influenza vaccine in older adults forecasts seroconversion. *Vaccine* **35**, 329–336.
- Pizzagalli, D.U., Latino, I., Pulfer, A., Palomino-Segura, M., Virgilio, T., Farsakoglu, Y., Krause, R., and Gonzalez, S.F. (2019). Characterization of the dynamic behavior of neutrophils following influenza vaccination. *Front. Immunol.* **10**. <https://doi.org/10.3389/fimmu.2019.02621>.
- Poovassery, J., and Moore, J.M. (2006). Murine malaria infection induces fetal loss associated with accumulation of Plasmodium chabaudi AS-infected erythrocytes in the placenta. *Infect. Immun.* **74**, 2839–2848.
- Rezende, R.M., Lopes, M.E., Menezes, G.B., and Weiner, H.L. (2019). Visualizing lymph node structure and cellular localization using ex-vivo confocal microscopy. *J. Vis. Exp.* <https://doi.org/10.3791/59335>.
- Sant, A.J., Dipiazza, A.T., Nayak, J.L., Rattan, A., and Richards, K.A. (2018). CD4 T cells in protection from influenza virus: viral antigen specificity and functional potential. *Immunol. Rev.* **284**, 91–105.
- Schudel, A., Francis, D.M., and Thomas, S.N. (2019). Material design for lymph node drug delivery. *Nat. Rev. Mater.* **4**, 415–428.
- Seth, S., Oberdorfer, L., Hyde, R., Hoff, K., Thies, V., Worbs, T., Schmitz, S., and Forster, R. (2011). CCR7 essentially contributes to the homing of plasmacytoid dendritic cells to lymph nodes under steady-state as well as inflammatory conditions. *J. Immunol.* **186**, 3364–3372.
- Shinnakasu, R., and Kurosaki, T. (2017). Regulation of memory B and plasma cell differentiation. *Curr. Opin. Immunol.* **45**, 126–131.
- Suan, D., Nguyen, A., Moran, I., Bourne, K., Hermes, J.R., Arshi, M., Hampton, H.R., Tomura, M., Miwa, Y., Kelleher, A.D., et al. (2015). T follicular helper cells have distinct modes of migration and molecular signatures in naive and memory immune responses. *Immunity* **42**, 704–718.
- Suh, W.K. (2015). Life of T follicular helper cells. *Mol. Cell.* **38**, 195–201.
- Swiecki, M., and Colonna, M. (2015). The multifaceted biology of plasmacytoid dendritic cells. *Nat. Rev. Immunol.* **15**, 471–485.
- Trub, M., Barr, T.A., Morrison, V.L., Brown, S., Caserta, S., Rixon, J., Ivens, A., and Gray, D. (2017). Heterogeneity of phenotype and function reflects the multistage development of T follicular helper cells. *Front. Immunol.* **8**, 489.
- Turner, J.S., O'Halloran, J.A., Kalaidina, E., Kim, W., Schmitz, A.J., Zhou, J.Q., Lei, T., Thapa, M., Chen, R.E., Case, J.B., et al. (2021). SARS-CoV-2 mRNA vaccines induce persistent human germinal centre responses. *Nature* **596**, 109–113.
- Turner, J.S., Zhou, J.Q., Han, J., Schmitz, A.J., Rizk, A.A., Alsoussi, W.B., Lei, T., Amor, M., McIntire, K.M., Meade, P., et al. (2020). Human germinal centres engage memory and naive B cells after influenza vaccination. *Nature* **586**, 127–132.
- Vella, L.A., Buggert, M., Manne, S., Herati, R.S., Sayin, I., Kuri-Cervantes, L., Bukh Brody, I., O'Boyle, K.C., Kaprielian, H., Giles, J.R., et al. (2019). T follicular helper cells in human efferent lymph retain lymphoid characteristics. *J. Clin. Invest.* **129**, 3185–3200.
- Vinuesa, C.G., Cook, M.C., Angelucci, C., Athanopoulos, V., Rui, L., Hill, K.M., Yu, D., Domasch, H., Whittle, B., Lambe, T., et al. (2005). A RING-type ubiquitin ligase family member required to repress follicular helper T cells and autoimmunity. *Nature* **435**, 452–458.
- Wikenheiser, D.J., and Stumhofer, J.S. (2016). ICOS Co-stimulation: friend or foe? *Front Immunol.* **7**, 304.
- Xu, Y., Fernandez, C., Alcantara, S., Bailey, M., De Rose, R., Kelleher, A.D., Zaunders, J., and Kent, S.J. (2013a). Serial study of lymph node cell subsets using fine needle aspiration in pigtail macaques. *J. Immunol. Methods* **394**, 73–83.
- Xu, Y., Phetsouphanh, C., Suzuki, K., Aggarwal, A., Graff-Dubois, S., Roche, M., Bailey, M., Alcantara, S., Cash, K., Siva, R., et al. (2017). HIV-1 and SIV predominantly use CCR5 expressed on a precursor population to establish infection in T follicular helper cells. *Front. Immunol.* **8**. <https://doi.org/10.3389/fimmu.2017.00376>.
- Xu, Y., Weatherall, C., Bailey, M., Alcantara, S., De Rose, R., Estaquier, J., Wilson, K., Suzuki, K., Corbeil, J., Cooper, D.A., et al. (2013b). Simian immunodeficiency virus infects follicular helper CD4 T cells in lymphoid tissues during pathogenic infection of pigtail macaques. *J. Virol.* **87**, 3760–3773.

Yu, D., Rao, S., Tsai, L.M., Lee, S.K., He, Y., Sutcliffe, E.L., Srivastava, M., Linterman, M., Zheng, L., Simpson, N., et al. (2009). The transcriptional repressor Bcl-6 directs T follicular helper cell lineage commitment. *Immunity* 31, 457–468.

Zaunders, J., Xu, Y., Kent, S.J., Koelsch, K.K., and Kelleher, A.D. (2017). Divergent expression of CXCR5 and CCR5 on CD4(+) T cells and the paradoxical accumulation of T follicular helper cells during HIV infection. *Front Immunol.* 8, 495.

Zaunders, J.J., Dyer, W.B., Munier, M.L., Ip, S., Liu, J., Amyes, E., Rawlinson, W., De Rose, R., Kent, S.J., Sullivan, J.S., et al. (2006). CD127+CCR5+CD38+++ CD4+ Th1 effector cells are an early component of the primary immune response to vaccinia virus and precede development of interleukin-2+ memory CD4+ T cells. *J. Virol.* 80, 10151–10161.

Zaunders, J.J., Munier, M.L., Kaufmann, D.E., Ip, S., Grey, P., Smith, D., Ramacciotti, T., Quan, D., Finlayson, R., Kaldor, J., et al. (2005). Early

proliferation of CCR5(+) CD38(+++) antigen-specific CD4(+) Th1 effector cells during primary HIV-1 infection. *Blood* 106, 1660–1667.

Zaunders, J.J., Munier, M.L., Seddiki, N., Pett, S., Ip, S., Bailey, M., Xu, Y., Brown, K., Dyer, W.B., Kim, M., et al. (2009). High levels of human antigen-specific CD4+ T cells in peripheral blood revealed by stimulated coexpression of CD25 and CD134 (OX40). *J. Immunol.* 183, 2827–2836.

STAR★METHODS

KEY RESOURCES TABLE

REAGENT or RESOURCE	SOURCE	IDENTIFIER
Antibodies		
CD3-PERCP-Cy5.5	BD Biosciences	Cat# 340949; RRID:AB_400190
CD56-APC	BD Biosciences	Cat# 341025; RRID:AB_400558
HLA-DR-FITC	BD Biosciences	Cat# 347363; RRID:AB_400291
CD20-APC-Cy7	BD Biosciences	Cat# 335794; RRID:AB_399972
CD123-PE	BD Biosciences	Cat# 340545; RRID:AB_400052
CD38-PE-Cy7	BD Biosciences	Cat# 335790; RRID:AB_399969
CD69-APC	BD Biosciences	Cat# 340560; RRID:AB_400523
CD8-APC-Cy7	BD Biosciences	Cat# 348793; RRID:AB_400383
CD16-BV421	BD Biosciences	Cat# 562874; RRID:AB_2716865
CD14-BV500	BD Biosciences	Cat# 561391; RRID:AB_10611856
CD4-BV605	BD Biosciences	Cat# 562658; RRID:AB_2744420
CD8-BV711	BD Biosciences	Cat# 563677; RRID:AB_2744463
CD19-BV786	BD Biosciences	Cat# 563325; RRID:AB_2744314
PD-1(CD279)-BV421	BD Biosciences	Cat# 562516; RRID:AB_11153482
ICOS(CD278)-BV711	BD Biosciences	Cat# 563833; RRID:AB_2738440
CD127-BV786	BD Biosciences	Cat# 563324; RRID:AB_2738138
CD25-BB515	BD Biosciences	Cat# 564467; RRID:AB_2744340
CD45-AlexaFlour700	BD Pharmingen	Cat# 560566; RRID:AB_1645452
Bcl6-AlexaFlour647	BD Pharmingen	Cat# 561525; RRID:AB_10898007
CD45RA-AlexaFlour700	BD Pharmingen	Cat# 560673; RRID:AB_1727496
CD25-PE-Cy5	BD Pharmingen	Cat# 555433; RRID:AB_395827
PD-1(CD279)-AlexaFlour647	BD Pharmingen	Cat# 560838; RRID:AB_2033988
Ki67-FITC	BD Pharmingen	Cat# 359604; RRID:AB_2562387
CXCR5(CD185)-PE/Dazzle594	Invitrogen	Cat# 356928; RRID:AB_2563689
CD134(OX40)-BV421	Invitrogen	Cat# 350014; RRID:AB_2564184
CD39-PE-Cy7	Invitrogen	Cat# 25-0399-42; RRID:AB_1582280
CCR5(CD195)-PE	Miltenyi Biotec	Cat# 130-117-356; RRID:AB_2733783
CCR5(CD195)-PE-Vio770	Miltenyi Biotec	Cat# 130-106-225; RRID:AB_2655917
Biological samples		
Human volunteers	TRESAX study	Approval Number HREC/17/SVH/20
Chemicals, peptides, and recombinant proteins		
Human FoxP3 Buffer Set	BD Pharmingen	Cat# 560098; RRID:AB_2869302
OptiLyse® C	Beckman Coulter	Cat# A11894
FACS Lyse Solution	Becton Dickinson	Cat# 349202; RRID:AB_2868862
Software and algorithms		
FlowJo version 10.7.1	Becton, Dickinson and Company, 2021	https://www.flowjo.com/
Prism version 8.4.2	GraphPad	https://www.graphpad.com/scientific-software/prism/

RESOURCE AVAILABILITY

Lead contact

Further information and requests for resources and reagents should be directed to and will be fulfilled by the lead contact, C. Mee Ling Munier (cmunier@kirby.unsw.edu.au).

Materials availability

This study did not generate new unique reagents.

Data and code availability

All data reported in this paper will be shared by the lead contact upon request. This paper does not report original code. Any additional information required to reanalyse the data reported in this paper is available from the lead contact upon request.

EXPERIMENTAL MODEL AND SUBJECT DETAILS

Study participants

Participants were healthy volunteers with previous history of influenza or influenza vaccination recruited at a single clinical site in Sydney, Australia. Baseline HAI titre confirmed previous exposure; mean = 44, IQR = 70, SD = 32. They were aged 18 years or older and had no prior history of immunodeficiency, immunosuppression or adverse reactions to vaccination. Prior to commencing the study, all participants provided informed written consent. This study was approved by St Vincent's Hospital Sydney Human Research Ethics Committee (HREC/17/SVH/20). Recruitment of participants occurred from 2018 to 2020 and participants received the annual tetra valent influenza vaccine appropriate to their year of recruitment. Details of the annual vaccines used in this study can be found in [Table](#) and the demographics of the participants are described in [Table S1](#). Bilateral axillary LN biopsies were conducted at baseline, prior to vaccination, and at day 5 post vaccination.

Table. Annual influenza vaccination details

Vaccine	Manufacturer	Antigen composition	Volume/antigen	Total volume of vaccine	Propagation mechanism	Route of injection
2018 season Influvac® Tetra (Influenza virus haemagglutinin)	Mylan	1. A/Michigan/45/2015 (H1N1)pdm09-like strain (A/Singapore/GP1908/2015, IVR-180) 2. A/Singapore/INFIMH-16-0019/2016 (H3N2)-like strain (A/Singapore/INFIMH-16-0019/2016, NIB-104) 3. B/Phuket/3073/2013-like strain (B/Phuket/3073/2013, wild type) 4. B/Brisbane/60/2008-like strain (B/Brisbane/60/2008, wild type)	15 µg/viral strain	0.5 mL	Fertilized hens' eggs from healthy chickens	Intramuscular
2019 season Influvac® Tetra (Influenza virus haemagglutinin)	Mylan	1. A/Michigan/45/2015 (H1N1)pdm09-like strain (A/Singapore/GP1908/2015, IVR-180) 2. A/Switzerland/8060/2017 (H3N2)-like strain (A/Brisbane/1/2018, NYMC BX-69A) 3. B/Colorado/06/2017-like strain (B/Victoria/2/87 lineage) (B/Maryland/15/2016, NYMC BX-69A) 4. B/Phuket/3073/2013-like strain (B/Yamagata/16/88 lineage) (B/Phuket/3073/2013, wild type)	15 µg/viral strain	0.5 mL	Fertilized hens' eggs from healthy chickens	Intramuscular

(Continued on next page)

Table. Continued

Vaccine	Manufacturer	Antigen composition	Volume/antigen	Total volume of vaccine	Propagation mechanism	Route of injection
2020 season Influvac® Tetra (Influenza virus haemagglutinin)	Mylan	1. A/Brisbane/02/2018 (H1N1)pdm09-like strain 2. A/South Australia/34/2019 (H3N2)-like strain 3. B/Washington/02/2019-like strain (B/Victoria lineage) 4. B/Phuket/3073/2013-like strain (B/Yamagata lineage)	15 µg/viral strain	0.5 mL	Fertilized hens' eggs from healthy chickens	Intramuscular

See also [Figure S1](#).

Lymph node fine needle biopsies

Human axillary LN FNBs were performed by a qualified, experienced radiologist and ultrasonographer at the Medical Imaging Department, St Vincent's Hospital, Sydney. Prior to influenza vaccination (baseline) and five days post vaccination (day 5), participants underwent bilateral FNB of axillary LNs and provided peripheral blood samples. After ultrasound identification of suitable bilateral axillary LNs local anaesthetic was administered and followed by four separate passes of a 25-gauge needle into each LN for cell collection. Cells were collected via capillary action; no aspiration was applied. Following each needle pass, the collected cells were transferred into a 15 mL tube (Falcon™, Becton Dickinson [BD], NJ, USA) containing culture media (Roswell Park memorial institute [RPMI-1640; Gibco®, Life Technologies, CA, USA] that was supplemented with 10% heat-inactivated 0.2 µm syringe-filtered fetal calf serum [FCS; Gibco®, Life Technologies]). Media from the tube was then drawn into the syringe and expelled to wash the needle of any residual cells. Each of the LN FNBs (left and right) was transferred to a separate 15 mL tube.

METHOD DETAILS

Flow cytometry

Immunophenotyping was performed on peripheral blood collected into 6mL sodium-heparin (Na-Hep) tubes (BD Biosciences, CA, USA) and FNB samples using the following conjugated antibodies: CD3-PERCP-Cy5.5 (clone SK7 [Leu-4]), CD56-APC (clone NCAM16.2), HLA-DR-FITC (clone L243), CD20-APC-Cy7 (clone L27), CD123-PE (clone 9F5), CD38-PE-Cy7 (clone HB7), CD69-APC (clone L78), CD8-APC-Cy7 (clone SK1) (BD); CD16-BV421 (clone 3G8), CD14-BV500 (clone M5E2), CD4-BV605 (clone RPPA-T4), CD8-BV711 (clone RPA-T8), CD19-BV786 (clone SJ25C1), PD-1(CD279)-BV421 (clone EH12.1), ICOS(CD278)-BV711 (clone DX29), CD127-BV786 (clone HIL-7R-M21), CD25-BB515 (clone 2A3) (BD Biosciences); CD45-AlexaFlour700 (clone HI30), Bcl6-AlexaFlour647 (clone K112-91), CD45RA-AlexaFlour700 (clone HI100), CD25-PE-Cy5 (clone M-A251), PD-1(CD279)-AlexaFlour647 (clone EH12.1), Ki67-FITC (clone B56) (BD Pharmingen); CXCR5(CD185)-PE/Dazzle594 (clone J252D4), CD134(OX40)-BV421 (clone Ber-ACT35) (BioLegend); CD39-PE-Cy7 (clone eBioA1) (Invitrogen); CCR5(CD195)-PE (clone REA245), CCR5(CD195)-PE-Vio770 (clone TM) (Miltenyi Biotec).

Antibodies used for immunophenotyping and enumeration of LN FNB and peripheral blood samples were titrated to stain <100µL of cell suspension. Cell suspensions were incubated with surface antibodies for 15 min at room temperature (RT) in the dark. To lyse red blood cells, 200µL of OptiLyse® C (Beckman Coulter) was added to the TruCount™ (BD Biosciences, CA, USA) tubes used for enumeration and 2mL of FACS Lyse Solution (Becton Dickinson) was added to all remaining tubes and were incubated for 10 min at RT in the dark. TruCount™ tubes were fixed with 0.5–1mL of 0.5% paraformaldehyde (PFA). Cells treated with FACS Lyse were washed with 2 mL of Dulbecco's phosphate-buffered saline supplemented with 0.5% bovine serum albumin (Sigma-Aldrich) and 0.1% sodium azide (Sigma-Aldrich) (PBA) by centrifugation at 335 x g for 7 min at 25°C. After the supernatant was discarded, cell pellets were resuspended in residual volume, and the remaining tubes were stained for intracellular or intranuclear proteins. The Human FoxP3 Buffer Set (BD Pharmingen™) was used for intracellular and intranuclear staining following surface antibody staining. Buffer A and Buffer C from the kit were made according to the manufacturer's instructions. Cell suspensions were washed with 2 mL of PBA at 400 x g for 7 min at 25°C, followed by incubation with intracellular or intranuclear antibodies of interest for 30 min at RT in the dark. 2 mL of

PBA was added to each tube for centrifugation at 400 x g for 7 min at 25°C. The supernatant was discarded, cells were resuspended in 150 µL of 0.5% PFA prior to analysis. All samples were run on a BD LSRII or BD Fortessa-X20 flow cytometer. FCS files were analysed using BD FlowJo version 10.7.1.

Functional assays

Antigen-specific CD4+ T cells were detected as previously described (Zaunders et al., 2009), identified by the expression of CD3, CD4, CD25 and CD134, following 44-h incubation with or without antigen. NaHep- anticoagulated peripheral blood was diluted with equal volume of Iscoves Modified Dulbecco's Medium (IMDM; Gibco, Life Technologies). 250µL of diluted blood was dispensed into a 48-well flat bottom tissue culture plate and incubated without antigen, polyclonal superantigen staphylococcal enterotoxin B (SEB; Sigma Aldrich), the combination of five influenza-A virus peptides (Miltenyi Biotec; described in Table) or Influenza A Viral Lysate (Zaunders et al., 2009) (Commonwealth Serum Laboratories). At the end of the 44-h incubation, 100ul of diluted blood was stained for cell surface proteins, as previously described (Zaunders et al., 2009; Xu et al., 2013b). Briefly, 100µL of diluted blood was incubated with surface antibodies for 15 min at RT in the dark. Red blood cells were lysed with 2mL of FACS Lyse Solution incubated for 10 min at RT in the dark. Cells were washed with 2mL of PBA by centrifugation at 335 x g for 7 min at 25°C. After the supernatant was discarded, cell pellets were resuspended in residual volume and fixed with 250µL of 0.5% PBA. A positive result in experimental antigen cultures was defined as greater than 20 cells that were CD25 + CD134+ and twice the background of the same population of the culture without antigen.

Table. Functional T cell assay stimulants

Culture	Antigen	Supplier	Catalog number	Stock concentration	Final concentration
No stimulation	N/A	N/A	N/A	N/A	N/A
Staphylococcal enterotoxin B (SEB)	(SEB)	Sigma-Aldrich	S4881	1mg/mL	1µg/mL; 0.25µg/250 µL culture
Influenza A H1N1 peptide pool	PepTivator Influenza A (H1N1) Haemagglutinin (HA)	Miltenyi Biotec	130-099-803	30nmol/mL	50µg/mL; 12.5µg/250 µL culture
	PepTivator Influenza A (H1N1) Neuraminidase (NA)	Miltenyi Biotec	130-099-806	30nmol/mL	50µg/mL; 12.5µg/250 µL culture
	PepTivator Influenza A (H1N1) Matrix Protein 1 (MP1)	Miltenyi Biotec	130-097-285	30nmol/mL	50µg/mL; 12.5µg/250µL culture
	PepTivator Influenza A (H1N1) Matrix Protein 2 (MP2)	Miltenyi Biotec	130-099-812	30nmol/mL	50µg/mL; 12.5µg/250 µL culture
	PepTivator Influenza A (H1N1) Nucleoprotein (NP)	Miltenyi Biotec	130-097-278	30nmol/mL	50µg/mL; 12.5µg /250µL culture

Quality control of LN FNB

Evaluation of viability of LN FNB samples can be seen in Figure S1. Samples were collected and cultured for 44 h post FNB procedure with no antigen and then viability of cells was assessed. FNB LN samples were stained with Live/Dead Aqua (BV510; Thermo Fischer), CD3 PERCP-Cy5.5 and CD4 BV605. Viability was 100% at 44 h post collection. Figure S1 is representative of 8 experiments using cells from both draining and contralateral LNs (n = 16). The median viability of these cells was 99.25% (range = 95.6%–100%).

NK cell, neutrophil and monocyte to lymphocyte ratio in LN and PB samples were used to determine presence of blood contamination (Figures S2A and S2B). The ratio of NK cells to lymphocytes was significantly higher in PB than in the FNB samples at both baseline and day 5 (Figure S2C). Similarly, a significant difference between PB and FNB samples was observed for neutrophil/lymphocyte (Figure S2D) and monocyte/lymphocyte (Figure S2E) ratios at both timepoints.

Lymphocyte subsets are present in different proportions in lymphoid tissue and peripheral blood due to the specialised functions of each compartment. Lymphocytes were defined as CD45+ cells, CD4+ T cells were defined as CD45+CD3+CD4+, CD8+ T cells were defined as CD45+CD3+CD8+ and B cells were defined as CD45+CD20+ cells. CD4+ T cells were the most common cell type detected in the lymphocyte compartments of both LN and PB (Figure S2G). CD4+ T cell frequencies were significantly higher in LN samples (draining LN median = 58.4%; contralateral LN median = 65.6%) than in PB (median = 50.9%; Figure S2G). CD8+ T cells made up the smallest proportion of lymphocytes in LN samples (draining LN median = 7.39%; contralateral LN median = 6.51%) and was significantly lower than in PB (median = 21.7%; Figure S2G). Finally, proportions of CD20+ B cells were significantly higher in LN samples (draining LN median = 19%; contralateral LN median = 16.7%) compared to PB (median = 11.7%; Figure S2G).

QUANTIFICATION AND STATISTICAL ANALYSIS

Statistics

For comparisons between responses at baseline and day 5 in draining and contralateral lymph nodes, Wilcoxon signed rank test was used to assess differences between sample pairs. Due to the paired nature of the data, day 5 samples were only included in this analysis if they had a baseline result available. For comparisons across three or more subsets (eg. draining, contralateral and peripheral blood samples), we first performed Friedman's test, testing for overall differences between the three or more subsets, and where this was statistically significant, we performed pairwise comparisons using Dunn's multiple comparison adjustment for p-values. Correlations between subsets were assessed using Spearman's non-parametric correlation coefficient. All statistical analyses were performed using Prism v8.4.2, and statistical significance was set at a two-sided $p < 0.05$. Statistical details of the analyses can also be found in the figure legends.